nature microbiology

SUPPLEMENTARY INFORMATION

ARTICLE NUMBER: 16068 | DOI: 10.1038/NMICROBIOL.2016.68

HIV–host interactome revealed directly from infected cells

Y Luo, EY Jacobs, TM Greco, KD Mohammed, T Tong, S Keegan, JM Binley, IM Cristea, D Fenyö, MP Rout, BT Chait & MA Muesing

DOI: 10.1038/NMICROBIOL.2016.68

Supplementary Figures and Tables

Supplementary Figure 1. Foreign epitope-tagged viruses are stable and without reversion over extended periods of outgrowth in culture.

Supplementary Figure 2. Although the immunoreactivity of the 3xFLAG tag is mainly restricted to the ER, the intracellular distribution of the tagged Env glycoprotein is not perturbed by 3xFLAG tag insertion.

Supplementary Figure 3. Immunoreactivity of the 3xFLAG epitope in Env-3xF infected CEM cells is diminished near the cell surface but present at points of syncytial contact between cells.

Supplementary Figure 4. The 3xFLAG epitope exhibits distinct immunoreactivity patterns during the early and late stages of infection.

Supplementary Figure 5. Foreign insertion within Env does not disrupt its overall glycosylation profile in infected producer cells.

Supplementary Figure 6. Neither the five amino acid (PmeI) nor the 35 amino acid 3xFLAG insertion disrupt the amount, stoichiometry or quality of the Env subunits incorporated into Env-3xF virions.

Supplementary Figure 7. Schematic diagram of I-DIRT MS methodology.

Supplementary Figure 8. Analysis of anti-FLAG affinity purified and natively eluted glycoprotein from Env-3xF infection.

Supplementary Figure 9. Construction and characterization of a set of HIV-1 indicator viruses.

Supplementary Figure 10. Insertion of 3xFLAG tag alters the mode of viral transmission.

Supplementary Figure 11. Schematic flow charts: TOR1AIP2 (LULL1); Env-mediated perturbation of host interactor NOTCH1.

Supplementary Figure 12. Detail of the I-DIRT ratios for the forward and reverse I-DIRT affinity isolations for the 3xFLAG-tagged HIV-1 Env protein.

Supplementary Figure 13. Detail of the I-DIRT ratios for the forward and reverse I-DIRT affinity isolations for the 3xFLAG-tagged HIV-1 Vif protein.

Supplementary Figure 14. Venn diagram comparison of Vif and Env host protein interactions identified by these analyses and that of Jäger et al.

Supplementary Figure 15. Comparison of the Vif and Env cellular interactors identified from cycling infection (Luo et al.) or from ectopic expression of individual viral proteins (Jäger et al.).

Supplementary Figure 16. Comparison cellular interactors identified by individualized ectopic expression of Vif and Env proteins (Jäger et al.) or from cycling viral infection (Luo et al.).

Supplementary Figure 17a-c. Raw data presentation.

Supplementary Table 1. Env host interactions: list of proteins classified as specific Env interactions by I-DIRT proteomic analysis.

Supplementary Table 2. Vif host and viral interactions: list of proteins classified as specific Vif interactions by I-DIRT proteomic analysis.

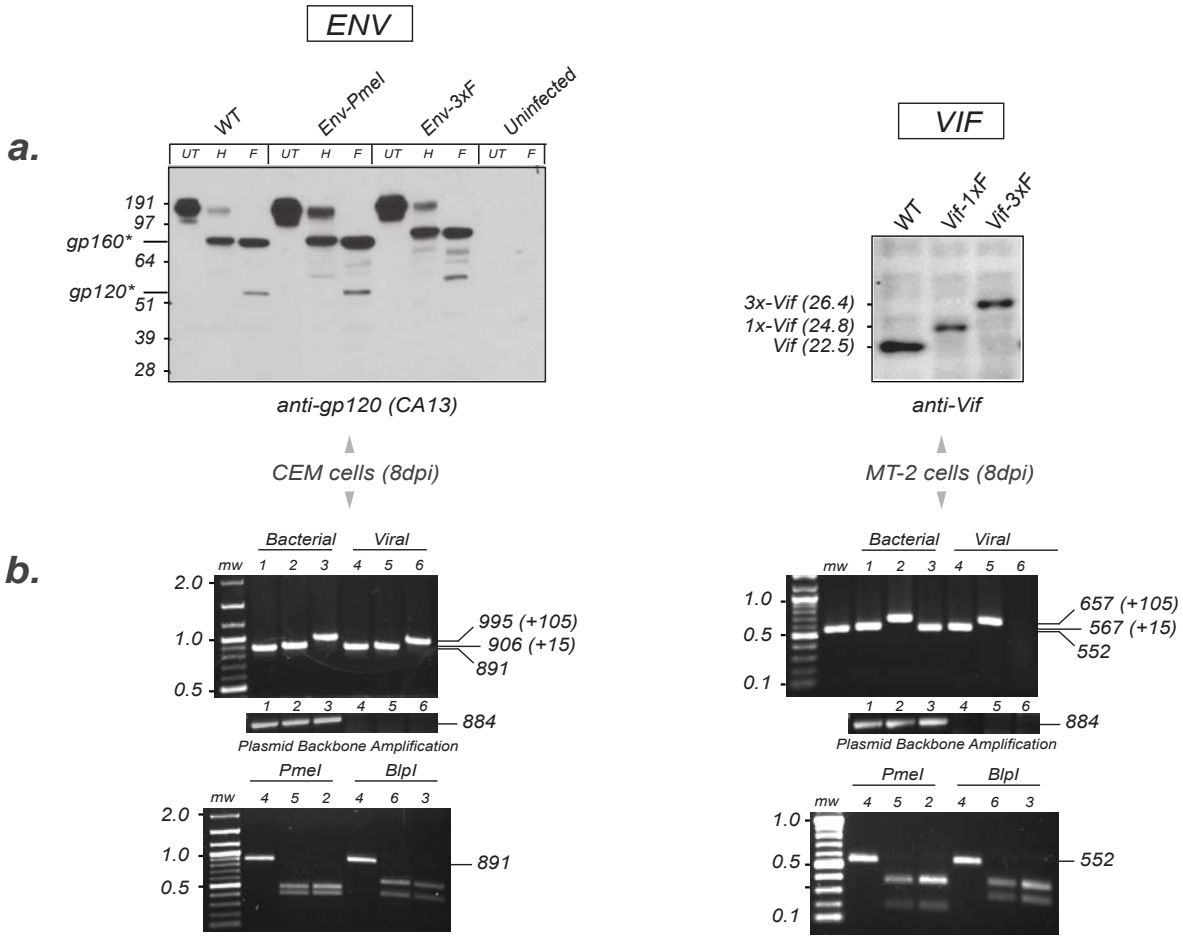

Supplementary Figure 1. Foreign epitope-tagged viruses are stable and without reversion over extended periods of outgrowth in culture. ***a.*** Western blot analysis of total lysate from infected cell cultures harvested ten days post infection (dpi) using antibodies against common epitopes of Env or Vif show no reduction in molecular weight of the tagged proteins. CEM cells were infected with untagged, Env-PmeI-inserted, Env-3xF viruses or left uninfected. Size differences of the gp160 Env proteins in the lysate before (untreated; UT) or after digestion with endonuclease H (H) or PNGaseF glycosidase digestion (F), the latter removing all N-linked glycans, were resolved in the upper left panel. The predicted molecular weight for deglycosylated WT gp160 (gp160*) and gp120 (gp120*) is 97.2 and 57.7 kDa, respectively and 101.2 kDa and 61.6 kDa for the 3xFLAG-tagged Env versions. Similarly, Vif restrictive MT-2 cells were infected with the untagged parental, Vif-1xF or Vif-3xF viral stocks. The calculated molecular weights of the WT and the modified Vif proteins are 22.5, 24.8 and 26.4 kDa, respectively. ***b.*** An alternative, confirmatory PCR assay based on the integrity of a specific gel mobility associated with tagged viral DNAs after extended rounds of infection also demonstrates the stability of the foreign insertions within Env- and Vif-tagged viruses. CEM (Env) or MT-2 (Vif) cells were independently infected with WT parental, Env-PmeI, Vif-PmeI, Env-3xF or Vif-3xF virus. After 12 days of viral outgrowth, total DNA was prepared from each infected culture, and cleaved with the bacterial DNA discriminating DpnI endonuclease prior to PCR amplification of the *vif* or *env* gene segment. Any residual bacterial DNA persisting in cells from the initial infection will be cleaved by the methylation-specific *DpnI*, resulting in the prevention of PCR amplification and contamination from DNA of bacterial origin. The resulting DNA fragments were either left uncut (top) or treated with restriction enzymes diagnostic with respect to the 15 base pair Tn7-mediated insertion (*PmeI*) or the 3xFLAG tag (*BlpI*) (bottom). For comparison, the proviral plasmid DNAs used to generate all viral stocks were amplified and treated as above. In addition, scoring for PCR amplification of a plasmid DNA backbone region confirms the absence of any bacterial plasmid DNA retained within the infected culture. Lane 1-3: PCR amplicon of proviral bacterial plasmid DNA; lane 4-6: PCR product of viral DNA 12 dpi; 1, 4: WT; 2, 5: 15 bp-inserted; 3, 6: 3xFLAG-tagged. Representative experiments were performed in duplicate.

DOI: 10.1038/NMICROBIOL.2016.68

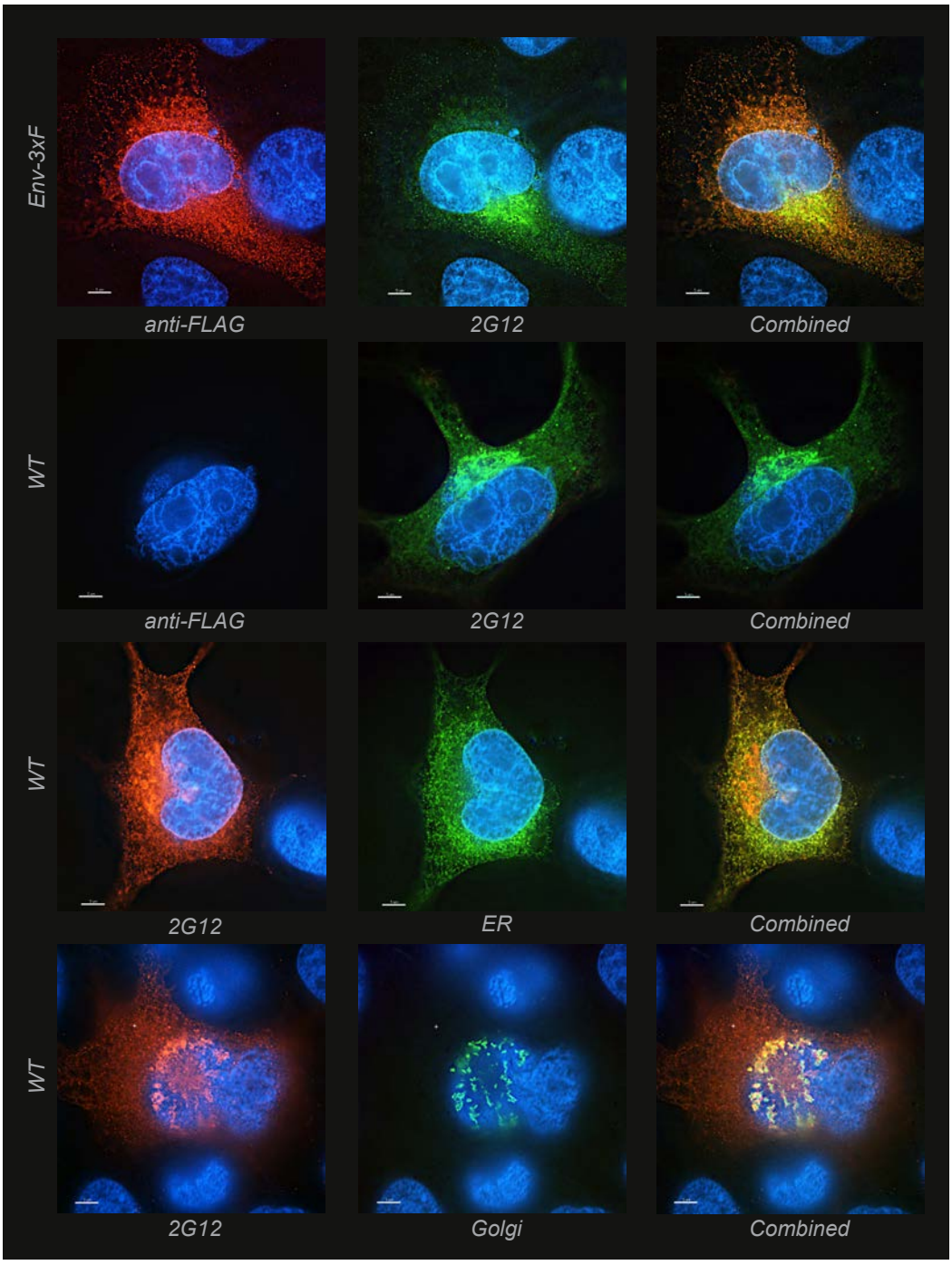

Supplementary Figure 2. Although the immunoreactivity of the 3xFLAG tag is mainly restricted to the ER, the intracellular distribution of the tagged Env glycoprotein is not perturbed by 3xFLAG tag insertion. HOS-CD4-Fusin cells were infected with the Env-3xF or WT virus and after an additional 48 hours of incubation, visualization of Env proteins performed by indirect immunofluorescence staining with anti-FLAG M2 followed by AlexaFluor 594 anti-mouse (red) or 2G12 followed by AlexaFluor 488 / 594 anti-human (green / red) secondary antibodies. Counter-staining for nuclear DNA was with Hoechst 33342 (blue). Baculoviruses encoding a specific fluorescent green probe (either CellLight ER-GFP or CellLight Golgi-GFP) were used to demarcate the boundaries of these organelles to confirm the global reactivity of the anti-Env 2G12 antibody. All images are representative of three independent experiments with almost all stained cells in the population illustrating the respective phenotype displayed. For all immunofluorescent studies shown, the bar denotes 5 μm.

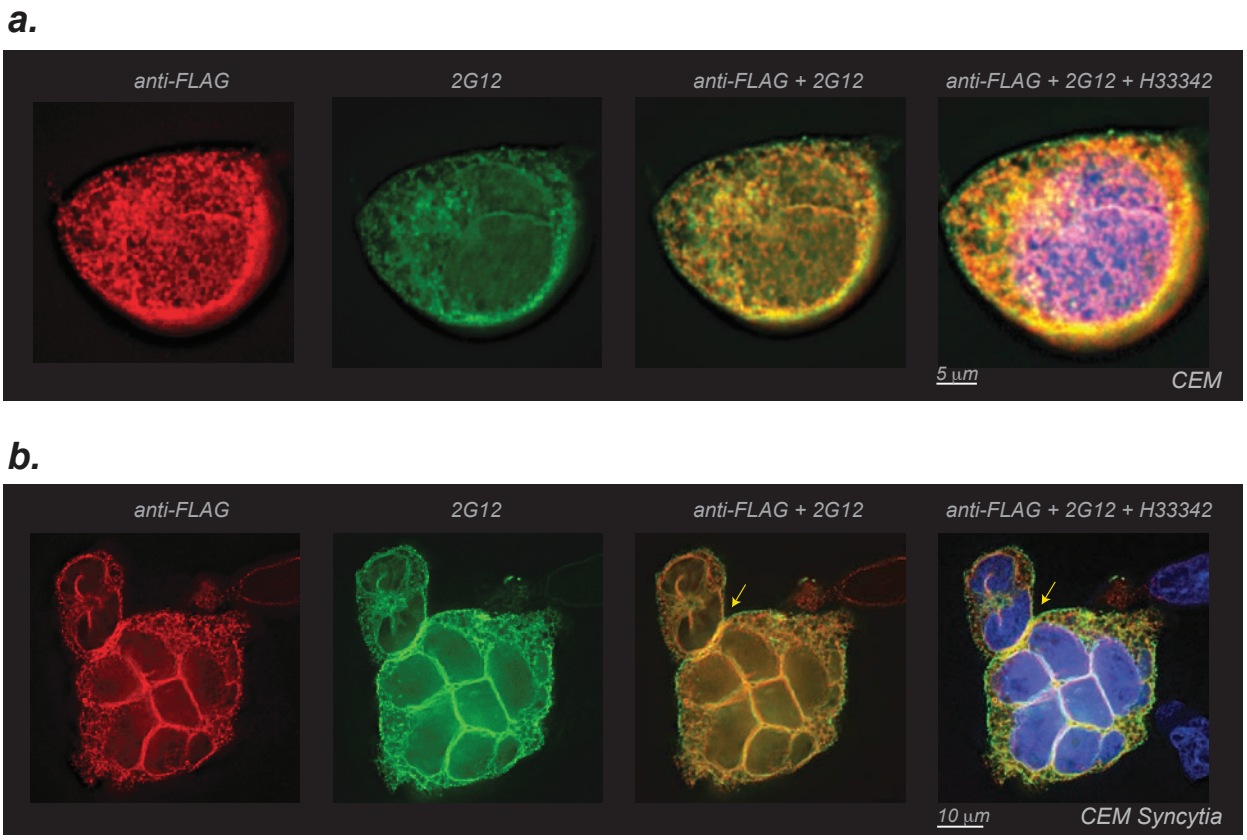

Supplementary Figure 3. Immunoreactivity of the 3xFLAG epitope in Env-3xF infected CEM cells is diminished near the cell surface but present at points of syncytial contact between cells. ***a.*** A single infected cell. ***b.*** Multinucleated syncytium of infected cells. Staining: anti-FLAG M2 followed by AlexaFluor 594 anti-mouse as secondary (red), 2G12 and AlexaFluor 488 anti-human (green), Hoechst 33342 counterstains nuclear DNA (blue). One slice from a set of deconvoluted set of 35 Z-sections is shown in both a. and b. The anti-FLAG staining pattern overlaps with that of 2G12 except for the outside perimeter of the cell. However, in the multinucleated syncytium (***b.***), the points of cell-cell contact appear reactive to both antibodies (i.e., yellow arrow). All images are representative of three independent experiments with almost all stained cells in the population illustrating the respective phenotype displayed. For all immunofluorescent studies shown, the bar denotes either 10 or 5 μm.

DOI: 10.1038/NMICROBIOL.2016.68

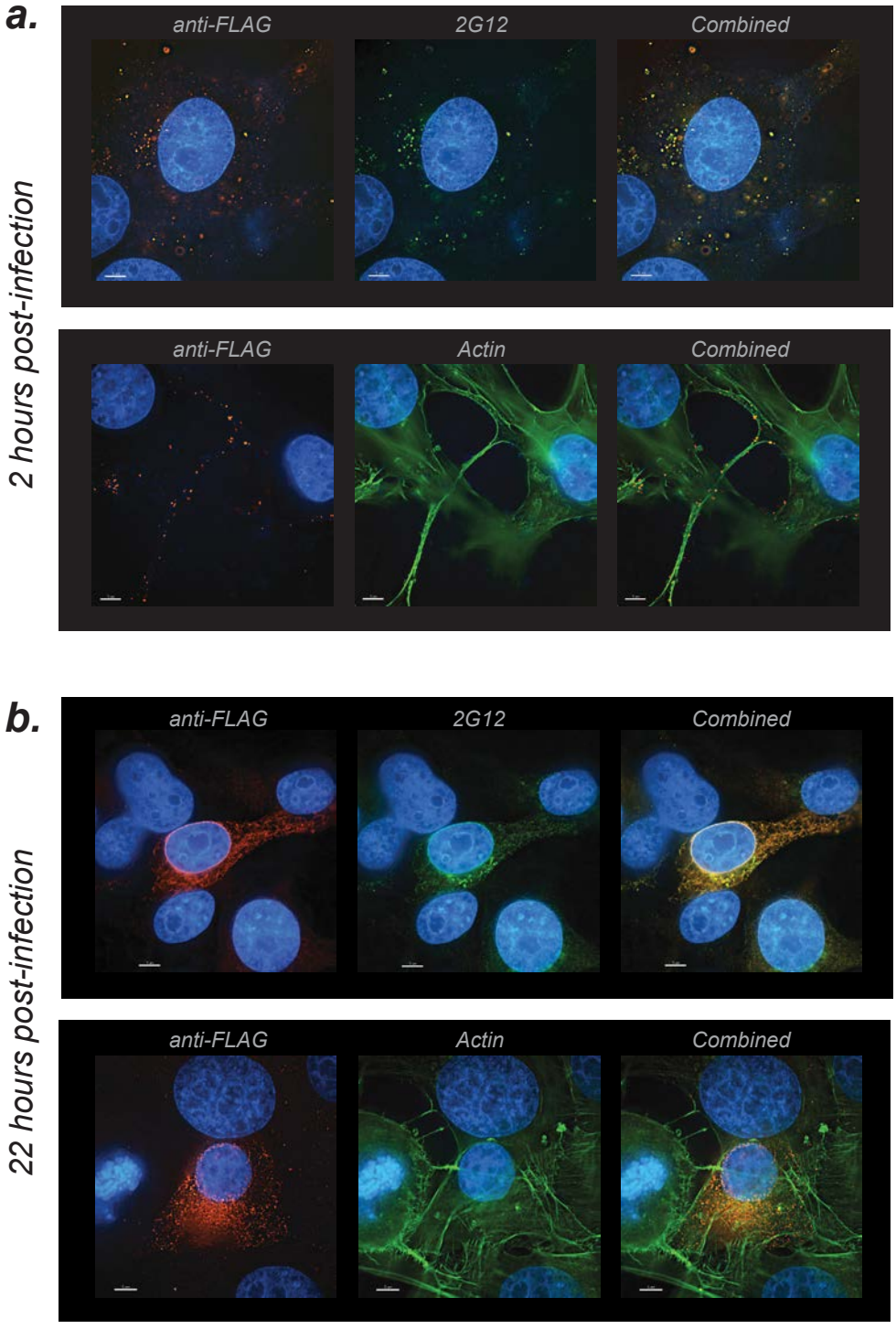

Supplementary Figure 4. The 3xFLAG epitope exhibits distinct immunoreactivity patterns during the early and late stages of infection. HOS-CD4-Fusin cells were infected with Env-3xF by spinoculation and cytochemically examined two different times after infection. ***a.*** 2 hpi, ***b.*** 22 hpi. Fluorescent staining conditions: anti-FLAG M2 mAb and AlexaFluor 594 anti-mouse secondary antibody (red), 2G12 and AlexaFluor 488 anti-human secondary antibody (green) or in a different set of experiments, green phalloidin stain for F-actin was used to assist in the determining of the location of the Env-3xF protein at each of the time points. All images are representative of three independent experiments with almost all stained cells in the population illustrating the respective phenotype displayed. For all immunofluorescent studies shown, the bar denotes 5 μm.

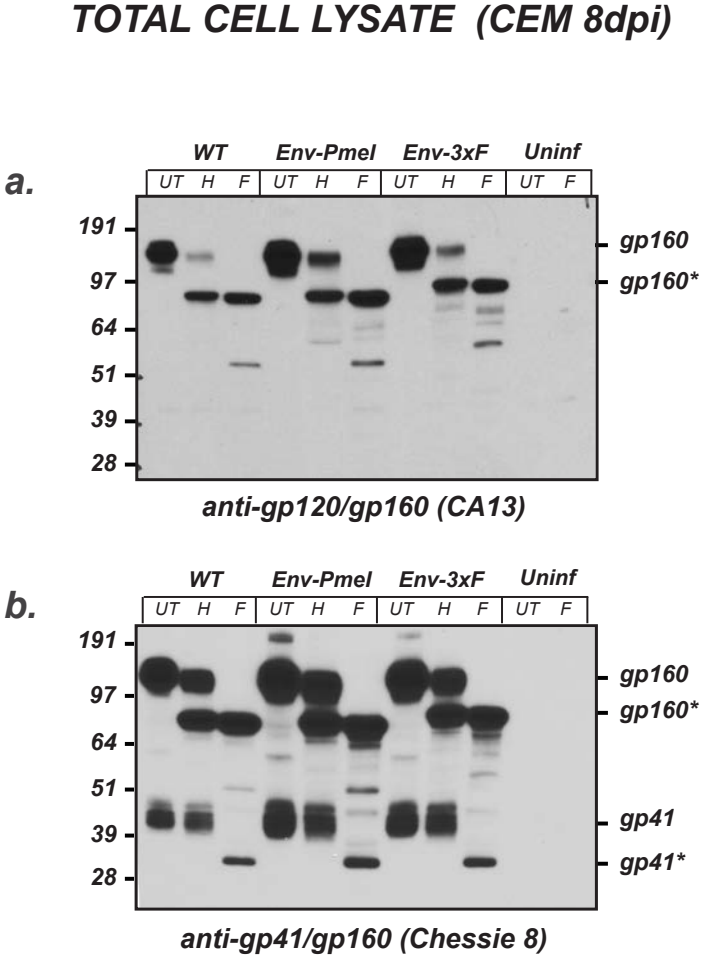

Supplementary Figure 5. Foreign insertion within Env does not disrupt its overall glycosylation profile in infected producer cells. Total cell lysates were prepared from CEM cultures infected with WT, Env-PmeI or Env-3xF at 8 dpi. An uninfected control cell lysate is also included. Samples were left untreated (UT) or incubated with either EndoH (H) or PNGaseF (F) glycosidase, then electrophoresed and probed in Western blot format using ***a.*** CA13 (ARP3119) specific for gp120 or ***b.*** Chessie 8 antibody that recognizes a gp41 epitope. (*), indicates the mobility expected of the deglycosylated counterparts of the Env proteins. Representative experiments were performed in triplicate.

DOI: 10.1038/NMICROBIOL.2016.68

VIRIONS

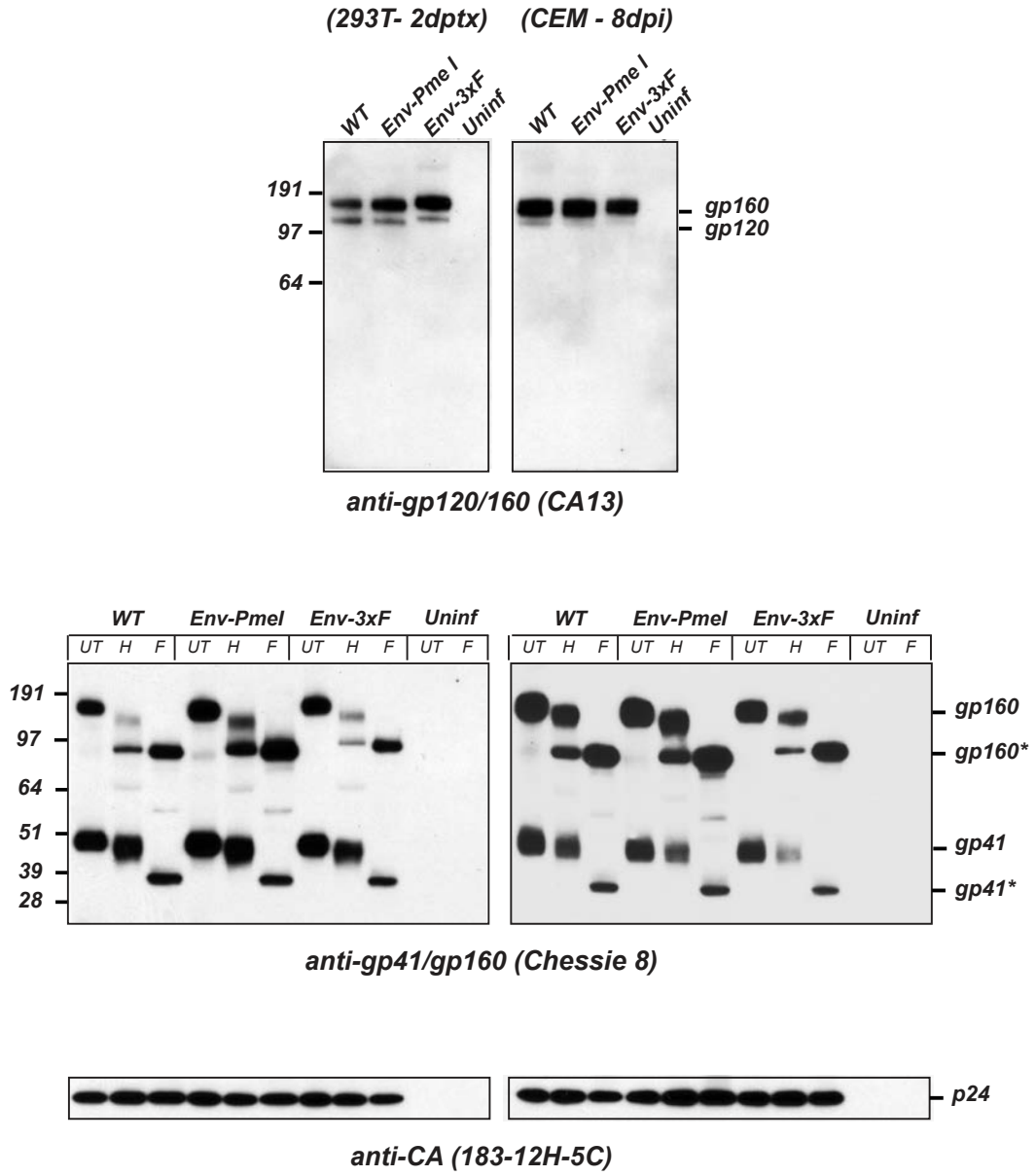

Supplementary Figure 6. Neither the five amino acid (PmeI) nor the 35 amino acid 3xFLAG insertion disrupt the amount, stoichiometry or quality of the Env subunits incorporated into Env-3xF virions. Viral particles were recovered and purified over sucrose from the supernatant of 293T cells transfected with the WT, Env-PmeI or Env-3xF proviral constructs (two days post-transfection, 2 dptx) or from the media of CEM cells infected with each of the respective viruses harvested 8 dpi. The virion preparations were normalized for p24 content and the samples were left untreated (UT) or incubated with either EndoH (H) or PNGaseF (F) glycosidase, electrophoresed and probed in Western blot format with antibodies specific for gp120, gp41 as in Supplementary Figure 5 or p24 (183-12H-5C). The ratio of gp160/gp120/gp41 normalized to p24 amount was comparable for all three viruses prepared from either transfected 293T or infected CEM cells. (*), indicates the mobility expected for the deglycosylated counterparts of the Env subunits. Representative experiments were performed in triplicate.

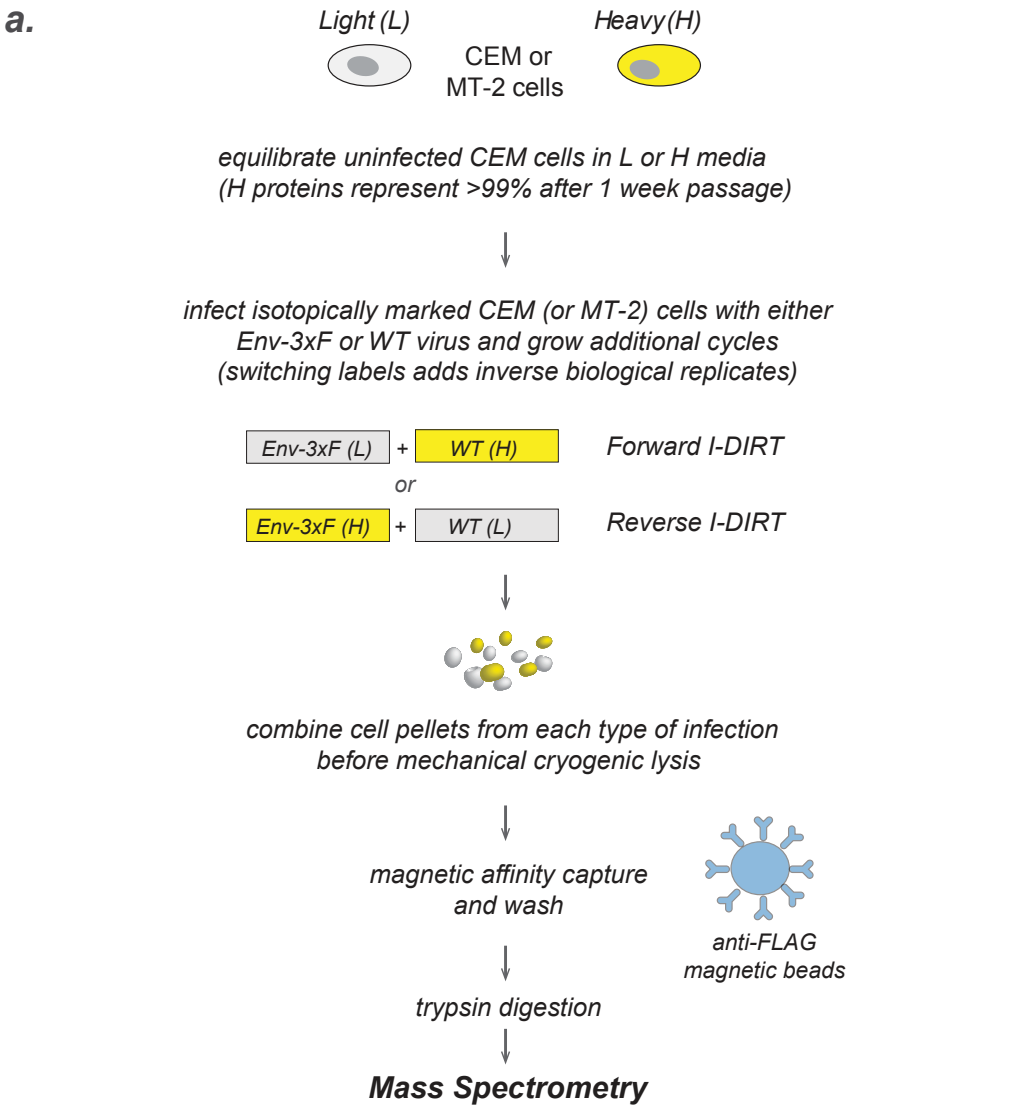

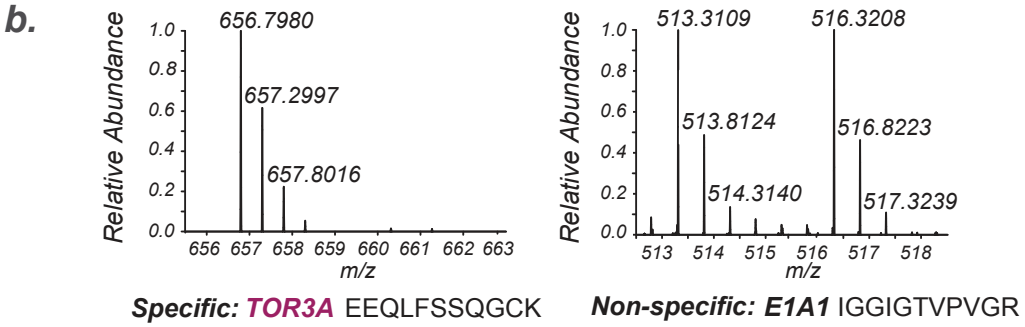

Supplementary Figure 7. Schematic diagram of I-DIRT MS methodology. ***a.*** The experimental flow of the technique is outlined. ***b.*** An example of the mass spectra of a peptide derived from a specific interacting protein (Tor3A) and from a non-specific interactor, E1A1. Proteins that exhibited high [L/(H+L)] ratios (or in the reverse isotope labeling, high [H/(H+L)]) were classified as specific interactions, while proteins with equal isotope incorporation were classified as nonspecific. The inclusion of a reverse isotope labeling experiment increased the robustness of the analysis, discriminated against possible exogenous contaminants and added an additional biological replicate.

DOI: 10.1038/NMICROBIOL.2016.68

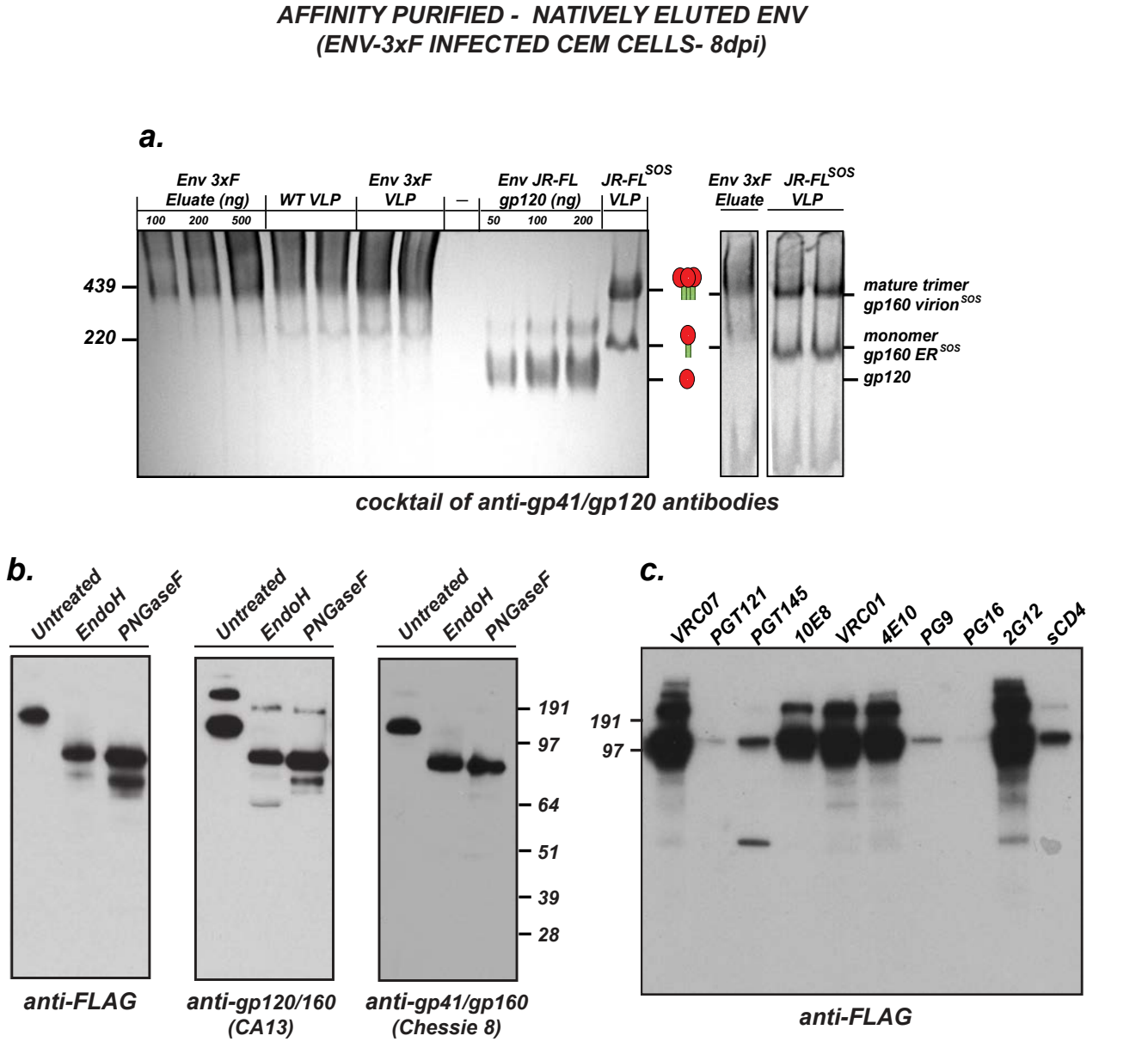

Supplementary Figure 8. Analysis of anti-FLAG affinity purified and natively eluted glycoprotein from Env-3xF infection. ***a.*** 3xFLAG peptide-eluted native Env protein recovered from Env-3xF infected cultures is predominantly trimerized, as shown by native gel electrophoresis probed with a cocktail of anti-gp41 and anti-gp120 antibodies (see Methods). The mobilities of purified gp120, monomeric and trimeric JR-FL Env SOS purified from VLPs (virus-like particles) control proteins are indicated. VLPs are pseudotyped with the indicated HIV-1 Env protein. ***b.*** Purified Env from Env-3xF infected cultures is proteolytically unprocessed and modified by high mannose addition but without further downstream glycosylation. Samples were left untreated or digested with the indicated endoglycosidase and probed in Western blot format as described in Supplementary Figures 5 and 6. ***c.*** The tagged Env trimer is recognized by a subset of bNAbs and soluble CD4 (sCD4-183, 2-domain) but not those antibodies that have epitopes near the site of 3xFLAG-tag insertion (amino acid 190, Figure 2A) or those that in part, require post-ER sugar modification for their recognition. The indicated antibody or sCD4 was individually covalently coupled to magnetic beads and incubated with the eluted Env overnight. The beads were then washed in binding buffer three times and the SDS eluted material electrophoresed and probed with anti-FLAG M2 antibody. Representative experiments were performed in duplicate.

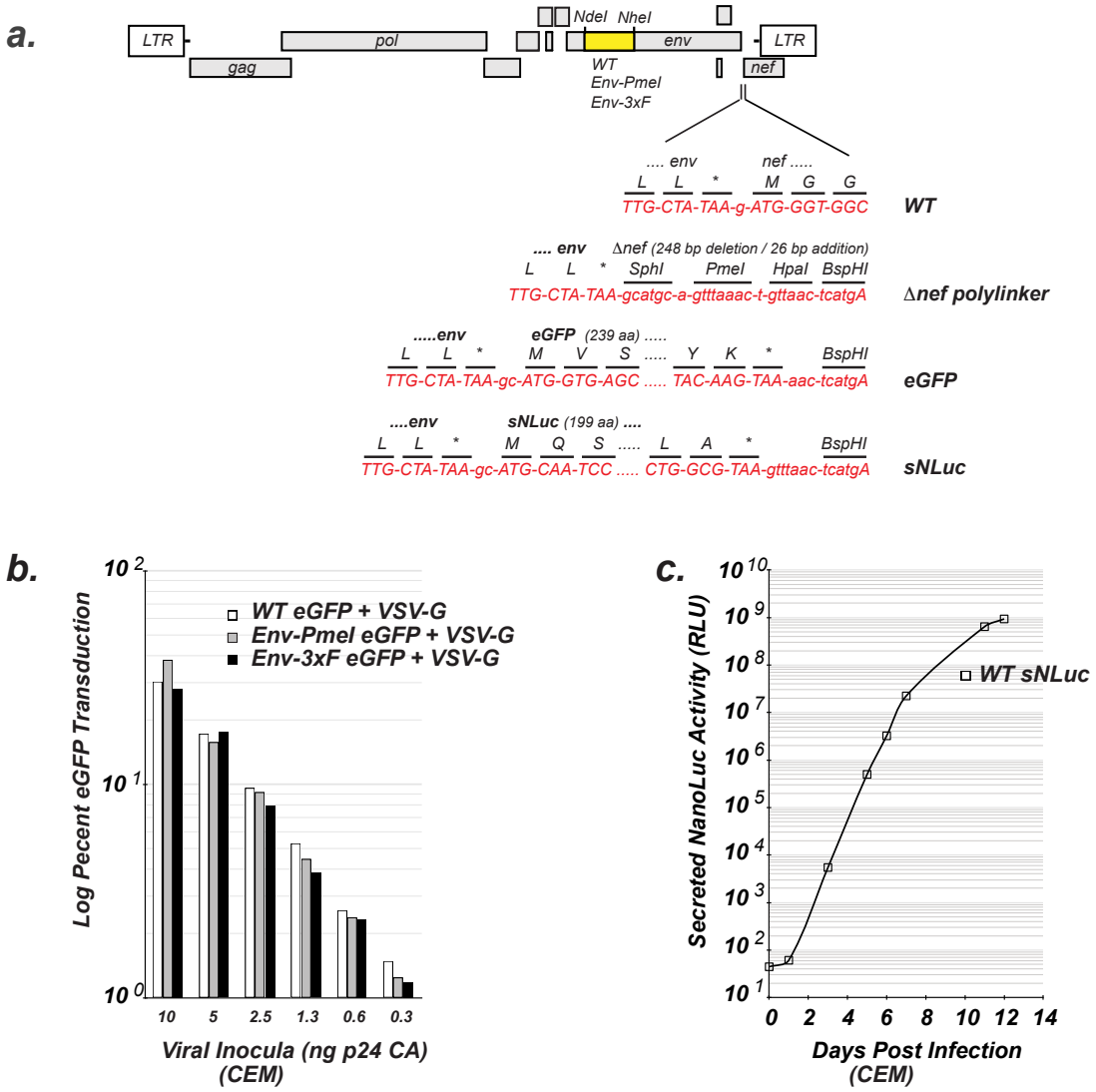

Supplementary Figure 9. Construction and characterization of a set of HIV-1 indicator viruses. ***a.*** Construction: enhanced green fluorescent (eGFP, Clontech) and secreted nanoluciferase (sNLuc, Promega) replication competent viral derivatives were constructed by first deleting 248 base pair (bp) of the nef gene coding region leaving the 3' LTR intact. The deletion was replaced by substitution with a 26 bp polylinker containing unique sites within the proviral DNA clone (Δnef polylinker), which was then used to accept the respective code for each of the small molecular weight indicator proteins. The DNA and amino acid sequences are shown for a small segment at the beginning and end of the eGFP and sNLuc derivatives. Both indicators utilize the natural ATG first codon of nef for the initiation of their translation. ***b.*** Single-step infection of WT, Env-PmeI and Env-3xF eGFP viral derivatives pseudotyped with the VSV-G Env (n=1) are linear with respect to input virus and are equally infectious at low moi. These results were used for calibration of the amount of input virus used to initiate the VSV-G pseudotyped infections of the sNLuc viral derivatives described in Supplementary Figure 10B. **C.** Viral growth curve of the WT sNLuc virus using a non-invasive, sensitive assay. The assay has wide dynamic range and measures the extent of viral propagation over several cycles of outgrowth. Approximately 5 ng p24 of the WT virus was used to initiate infection of a 5 ml culture of 1 x 10e6 CEM cells and after 1 hr incubation at 37º C the cells were washed three times in PBS, media added back, a 0 time point taken and the medium scored for sNLuc activity (RLU, relative light units) over the course of 12 days (n=1). Although the growth curve is adjusted for the dilution of the culture from each split ratio over the course of the study, the dynamic range in terms of absolute RLUs is 4 x 10e1 (day 0) to 10e7 (day 12). Secreted nanoluciferase provides an easy assay particularly well suited for infected suspension cell cultures that exhibit extensive syncytia formation (i.e., CEM) confounding accurate monitoring of viral growth.

DOI: 10.1038/NMICROBIOL.2016.68

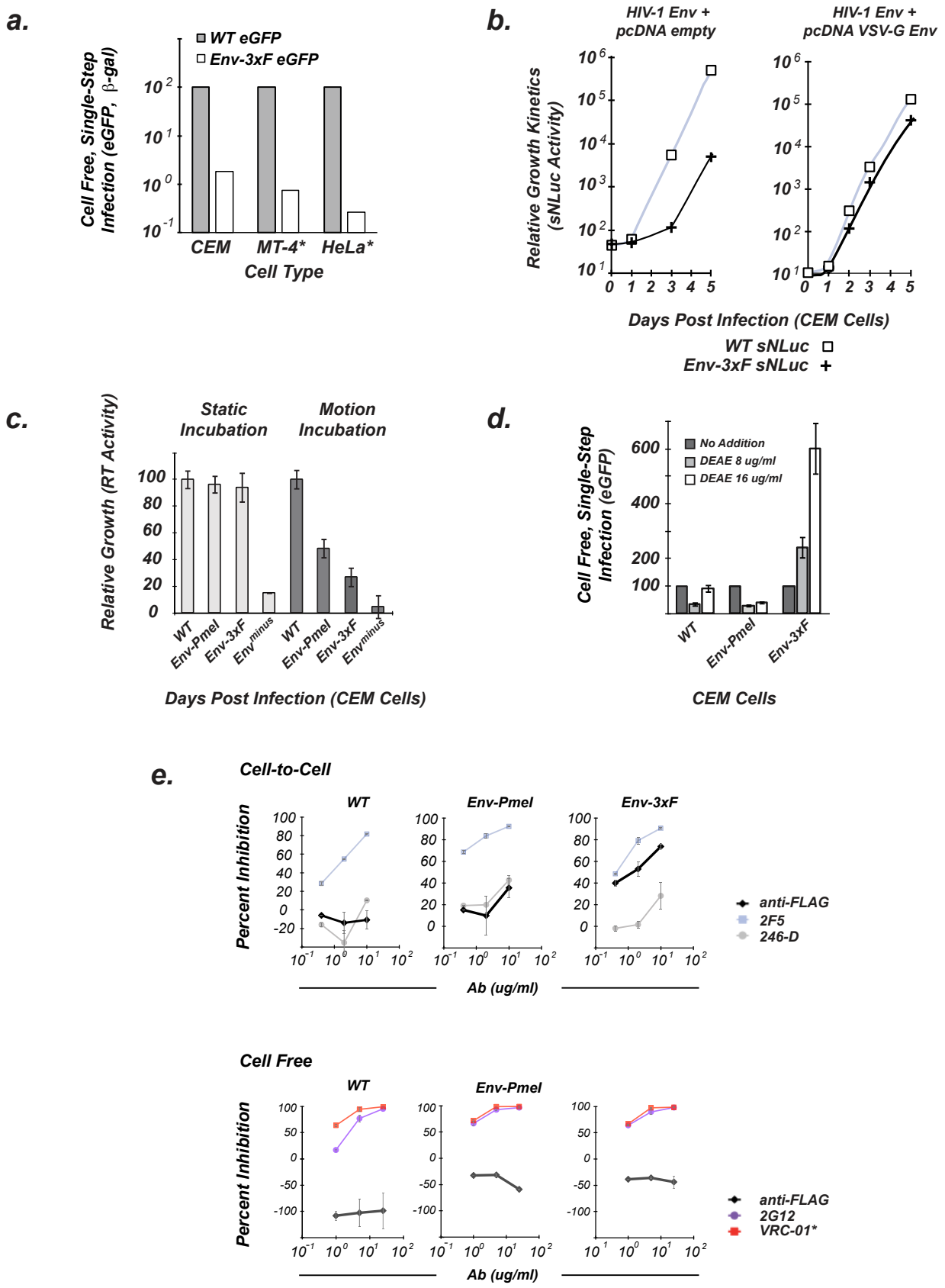

Supplementary Figure 10 *(see legend on next page)*

Supplementary Figure 10 (previous page). Insertion of 3xFLAG tag alters the mode of viral transmission. ***a.*** Env-3xF is remarkably defective for cell free infection compared to the WT virus. Under conditions of cell free infection, the growth of Env-3xF is highly compromised and exhibits about a 100-fold decrease in infection efficiency compared to the WT virus during single step infection of various types of susceptible cells. Viral eGFP derivatives of WT or Env-3xF (Supplementary Figure 9) were normalized for p24 content and used to infect three different cell types at a low moi and the extent of successful infection ascertained by scoring for GFP transduction by flow cytometry using lymphoid cell lines CEM and MT-4-GFP (MT-4*) or measurement of β-galactosidase activity after infection of the HeLa-derived, HIV reporter cell line, TZM-bl (HeLa*). Under these conditions, approximately 20% of both the CEM and MT-4 cells within the population were infected with the WT virus. The results presented are relative to the WT infection, which is arbitrarily set at a value of 100 (n=2). ***b.*** Env-3xF is poorly transmitted by cell free infection but is nearly as efficient as WT viral growth kinetics when infection is normalized for the efficiency of the first round of infection. Consistent with the finding in ***a.***, compared to the WT virus, Env-3xF is also delayed in achieving exponential growth during cycling infection that at later time points also results in a loss of up to two orders of magnitude of viral growth after 5 dpi (***b***, left plot). Paradoxically, although the Env-3xF virus is profoundly inefficient in establishing infection by the cell free route, it is able to proficiently expand in culture over a two week period in CEM cells suggesting the possibility that a major route of sustained infection for the Env-3xF virus in this cell type is via cell-to-cell contact and transmission through CEM suspension culture. Thus, we developed a system to bypass the initial infectious step using *super-pseudotyped* viruses containing the VSV-G envelope, setting to equivalence the number of cells infected for each type of reporter virus (Supplementary Figure 9B). Viral stocks were prepared as super-pseudotyped versions: WT and modified Env eGFP proviral DNAs were each co-transfected with a pcDNA VSV-G Env expression vector or as a control, pcDNA empty. Stocks were then normalized for RT activity and p24 CA content and used to infect CEM cells (***b***, right panel) and tracked across 5 dpi using sNLuc activity as a surrogate marker for viral expansion (n=2). ***c.*** The growth of modified viruses in CEM cells are inhibited under incubation conditions of constant motion. WT is set to 100 for each respective growth condition. ***d.*** DEAE-dextran facilitates Env-3xF cell free infection of CEM cells. Values are relative to the no addition control infection set at 100 for each virus. The set of eGFP-marked viruses were used for this analysis. ***e.*** Env-3xF cell-to-cell, but not cell free transmission can be neutralized by the anti-FLAG mouse mAb, M2. A set of eGFP-marked viruses were super-pseudotyped with the VSV-G envelope protein and used to infect CEM cells such that approximately 1% of the cells were infected. 18 hpi, an aliquot of uninfected CEM cells were added in the presence of increasing concentrations of the indicated human or mouse monoclonal antibody, the percent of GFP positive cells relative to the no antibody control assessed after an additional 3 days of further incubation. Antibody inhibition of cell free transmission was measured in during single-step infection of HeLa* indicator cells (see panel a) against the indicated antibody. In this experiment, viral infectivity was normalized to 5% for all viral stocks and the inoculum then incubated with antibody before infection of the indicator cell line. To facilitate figure display, the titration curve for VRC01* is an order of magnitude lower in concentration than that of all other comparator antibodies.

DOI: 10.1038/NMICROBIOL.2016.68

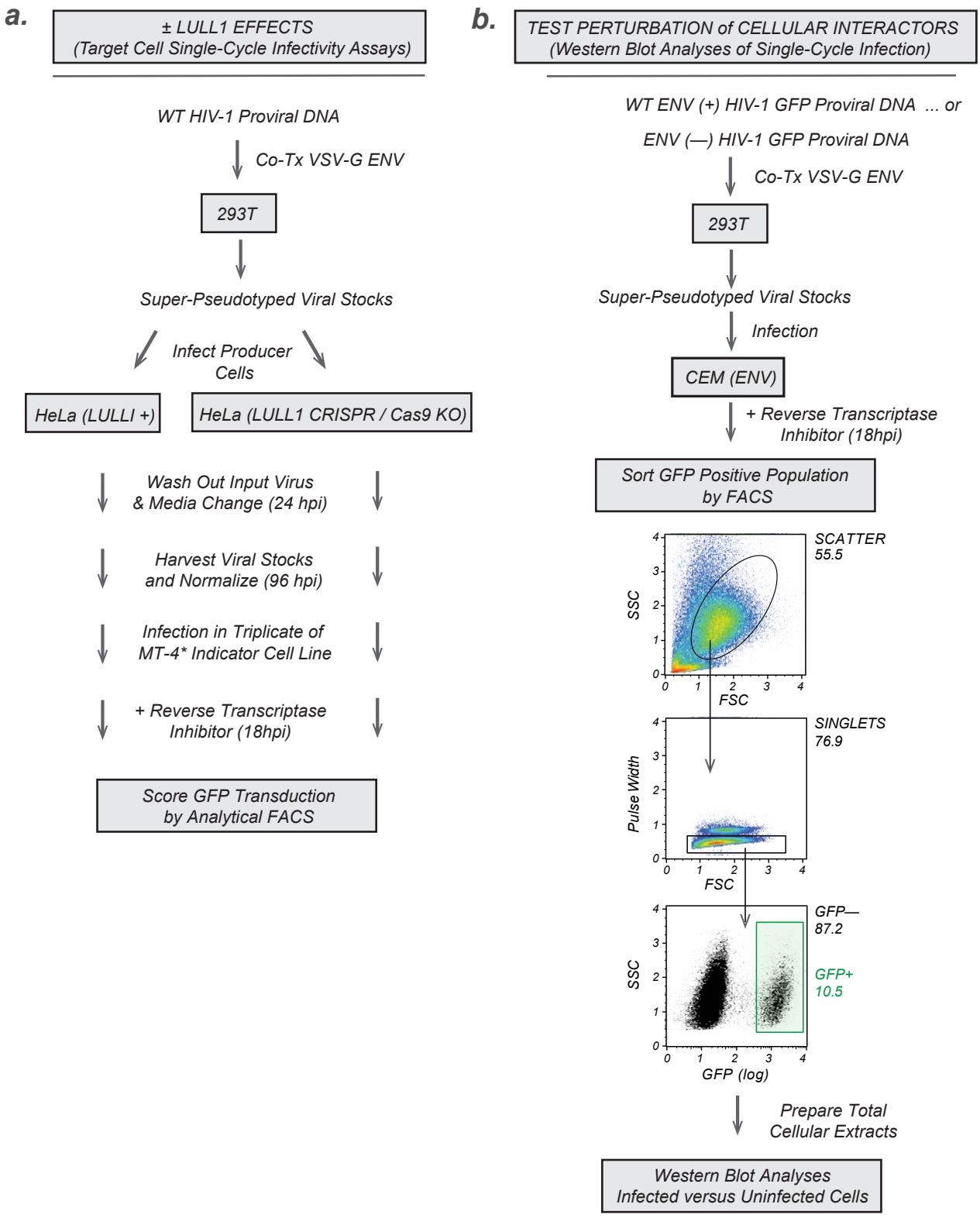

Supplementary Figure 11. Schematic flow charts to determine: ***a.*** Contribution of TOR1AIP2 (LULL1) to viral infectivity. ***b.*** Preparation of differentially infected cells (CEM) to examine the potential for Env-mediated perturbation of NOTCH1, a host interactor identified by I-DIRT analyses. The experimental specifics of these protocols can be found in the Methods.

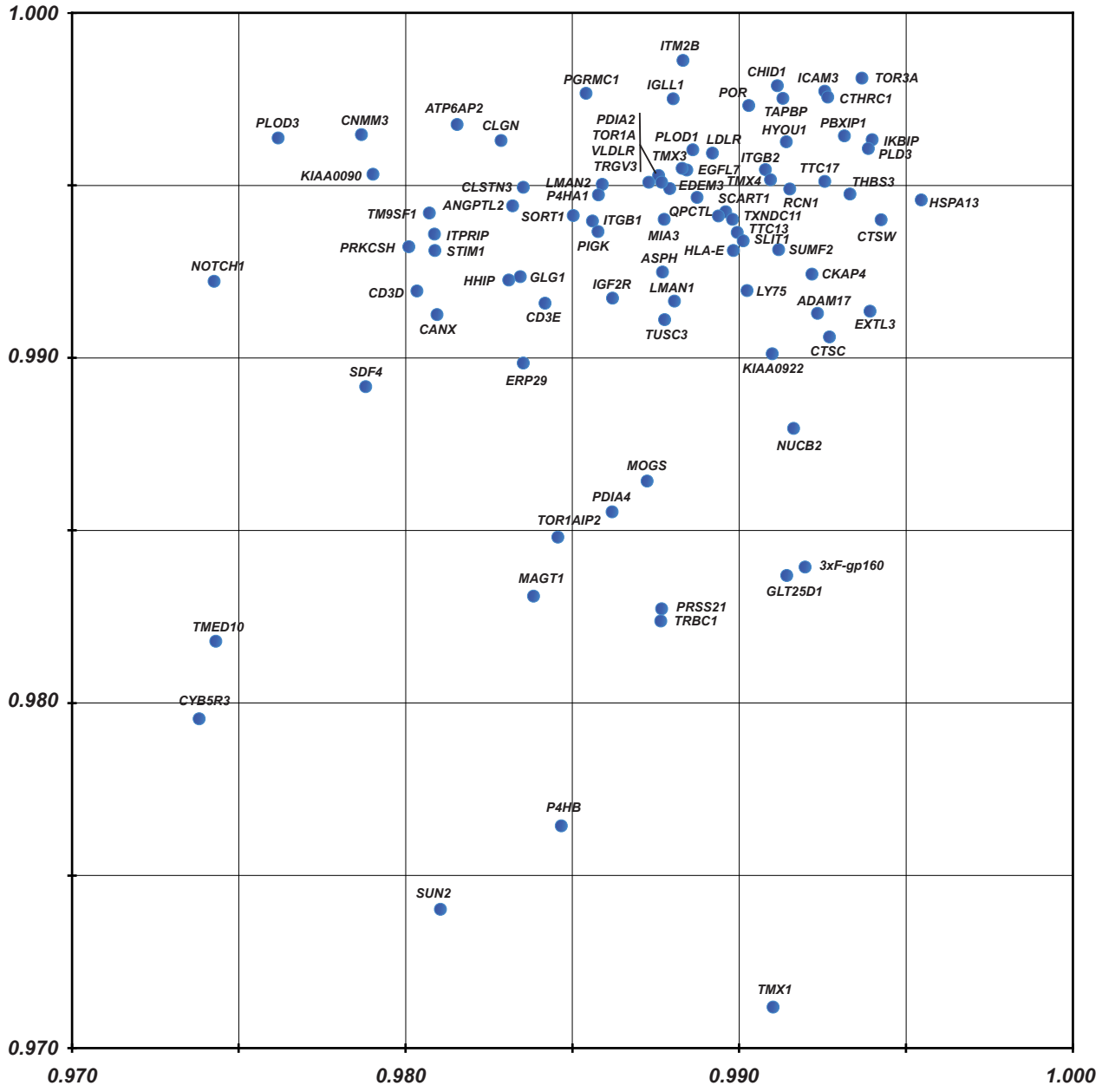

Supplementary Figure 12. Detail of the I-DIRT ratios for the forward and reverse I-DIRT affinity isolations for the 3xFLAG-tagged HIV-1 Env protein. The identity and relative placement of all specific (>0.97) Env interactors. Y axis: Reverse I-DIRT ratio; X-axis: Forward I-DIRT ratio.

DOI: 10.1038/NMICROBIOL.2016.68

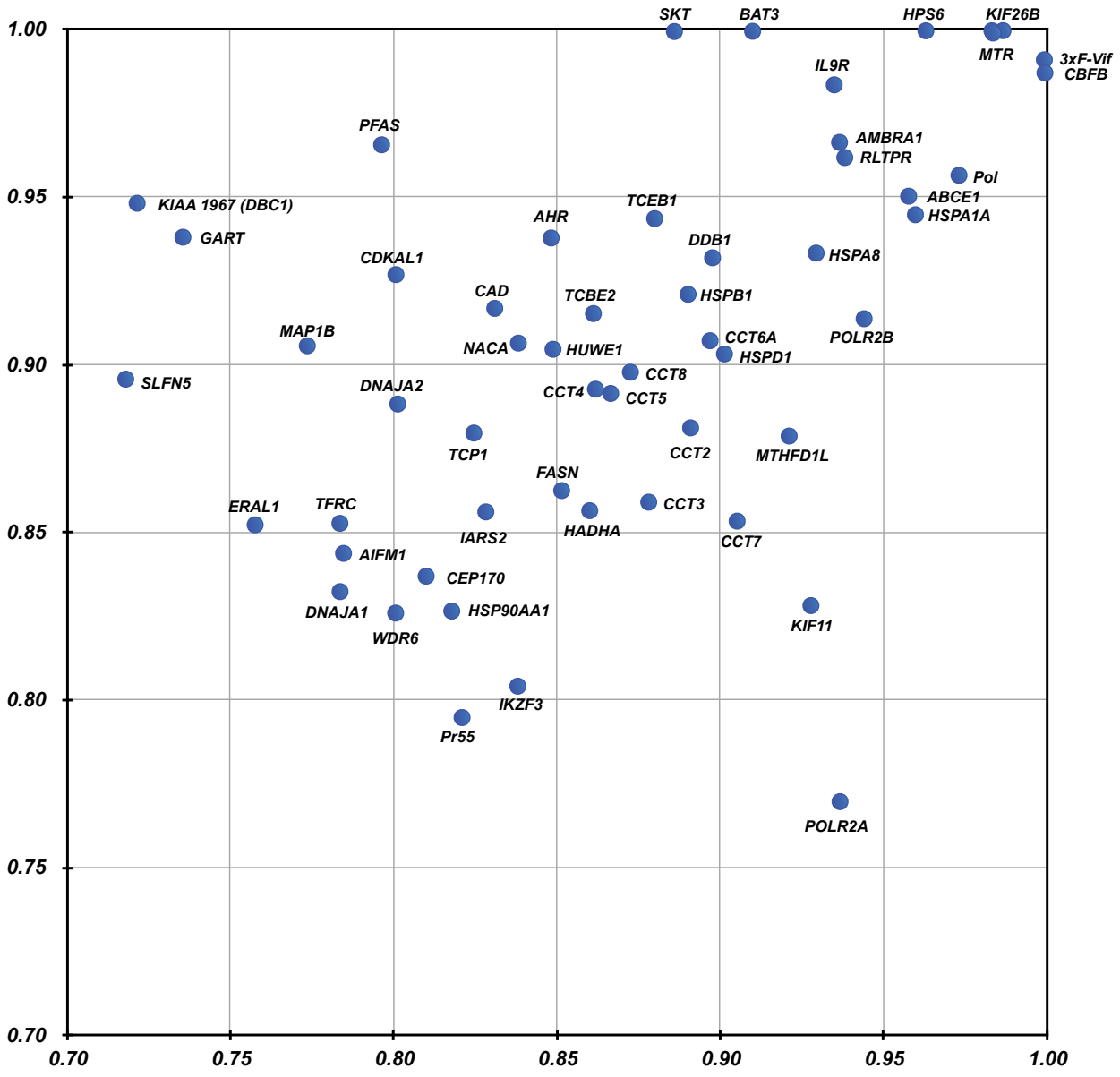

Supplementary Figure 13. Detail of the I-DIRT ratios for the forward and reverse I-DIRT affinity isolations for the 3xFLAG-tagged HIV-1 Vif protein. The identity and relative placement of all specific (>0.70) Vif interactors. Y axis: Reverse I-DIRT ratio; X-axis: Forward I-DIRT ratio.

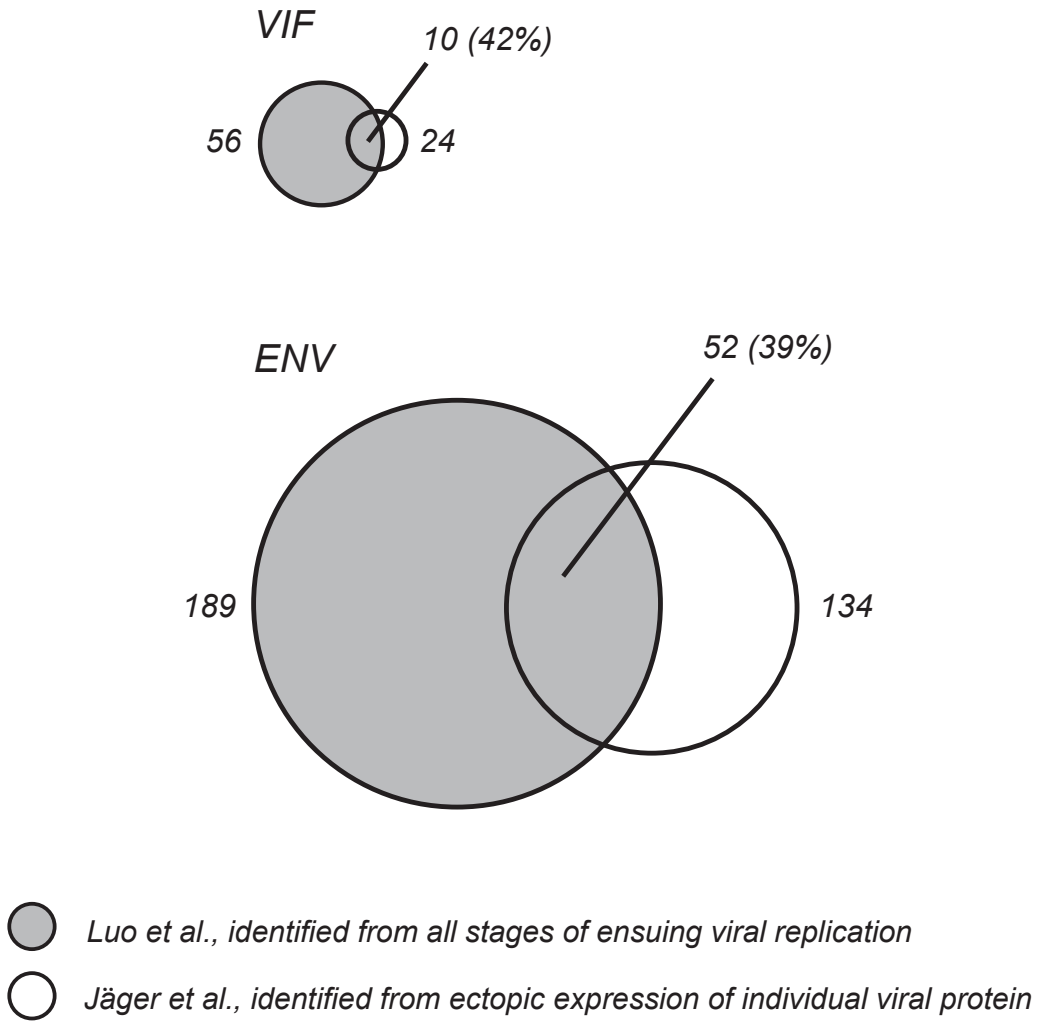

Supplementary Figure 14. Venn diagram comparison of Vif and Env host protein interactions identified by these analyses and that of Jäger et al. Number of interactors identified (see also Supplementary Figures 14, 15 and Supplementary Tables 1 and 2) for each viral protein and those overlapping between the two data sets. The percent of factors found by both groups is given with reference to the Jäger et al. study (i.e., shared identities divided by those in total by Jäger et al.).

DOI: 10.1038/NMICROBIOL.2016.68

Interactomes (Luo)

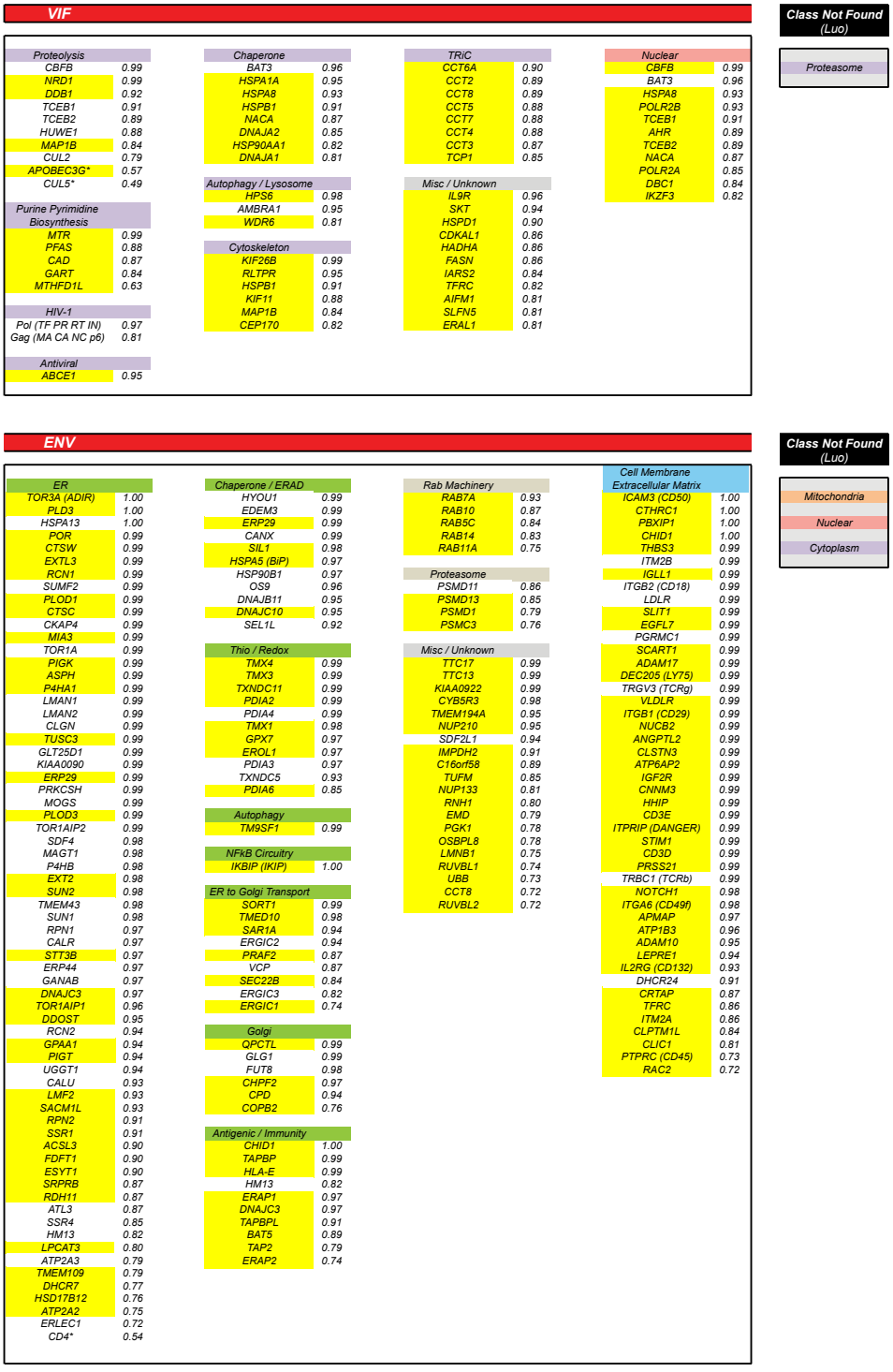

Supplementary Figure 15. Comparison of the Vif and Env cellular interactors identified from cycling infection (Luo et al.) or from ectopic expression of individual viral proteins (Jäger et al.). All proteins identified by I-DIRT analysis are listed (along with their averaged forward and reverse I-DIRT quotient). Yellow highlight, host proteins only identified by I-DIRT analyses of immunoprecipitations from ensuing infected cell culture. Unhighlighted, host proteins identified by both approaches. Asterisk (APOBEC3G, CUL5, CD4), proteins found to be in dynamic association with the viral machinery. Disparate functional and/or subcellular localization classes are listed to the right.

Interactomes (Jäger)

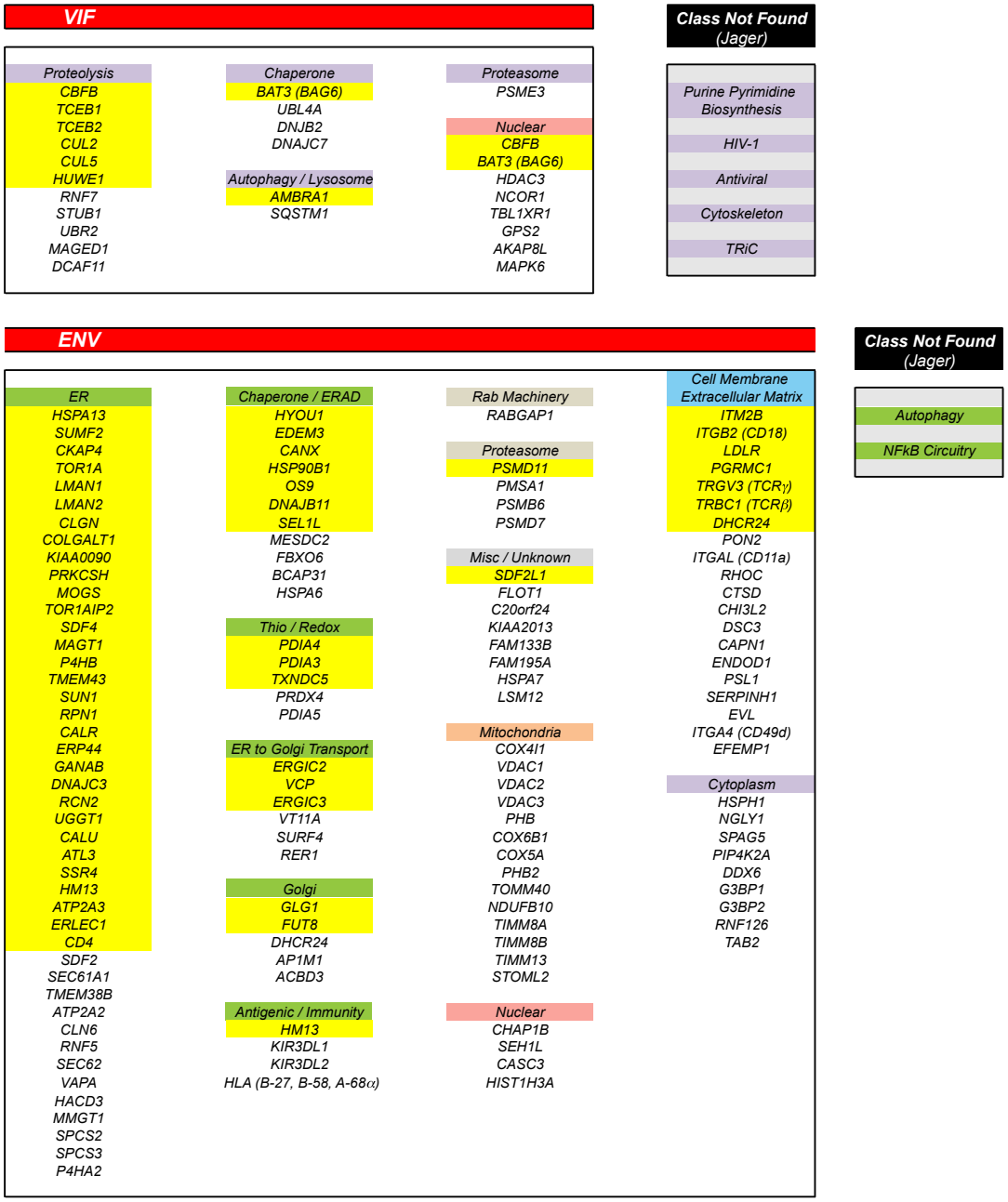

Supplementary Figure 16. Comparison cellular interactors identified by individualized ectopic expression of Vif and Env proteins (Jäger et al.) or from cycling viral infection (Luo et al.). All proteins identified by individualized ectopic expression of Vif and Env proteins are listed. Those shared also by I-DIRT identification from infected cell culture are shown in yellow highlight and listed along with their averaged forward and reverse I-DIRT quotient. Disparate cellular functional and/or subcellular localization classes are listed to the right.

DOI: 10.1038/NMICROBIOL.2016.68

Figure 1b

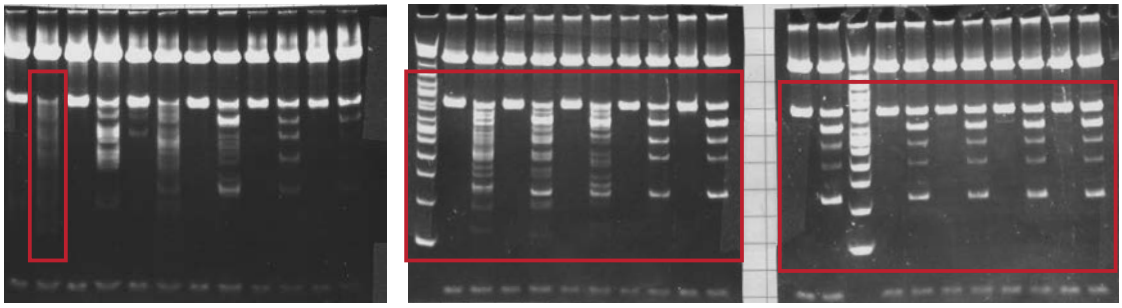

Figure 5a

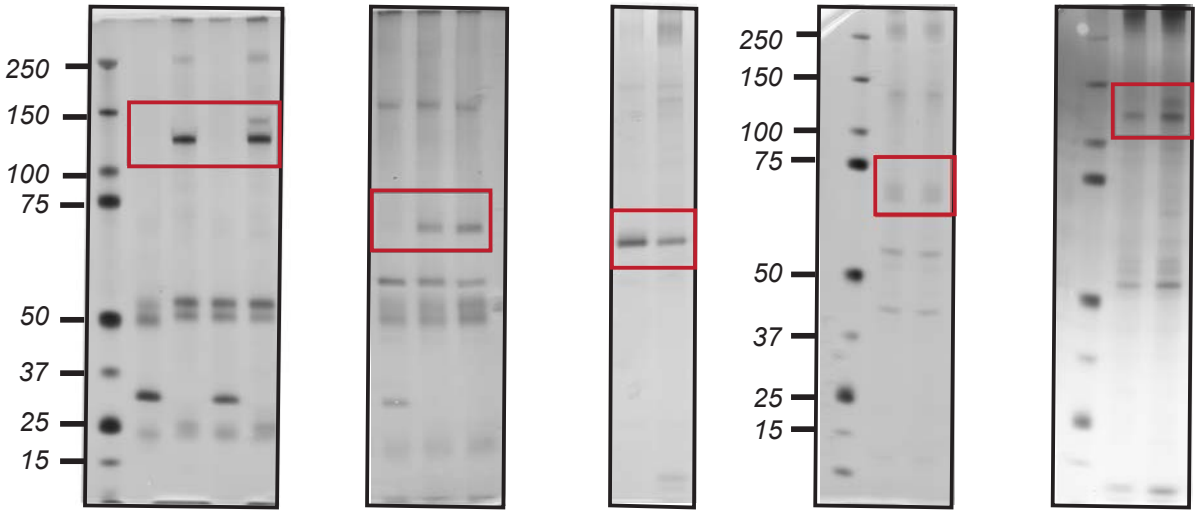

Figure 5d

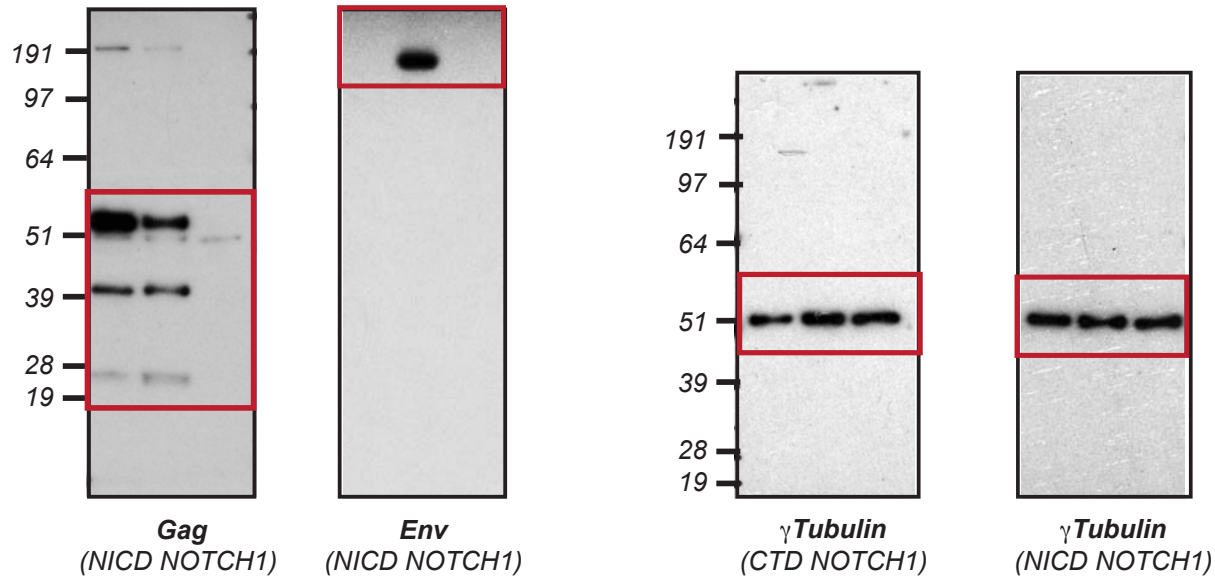

Supplementary Figure 17a. Raw data presentation

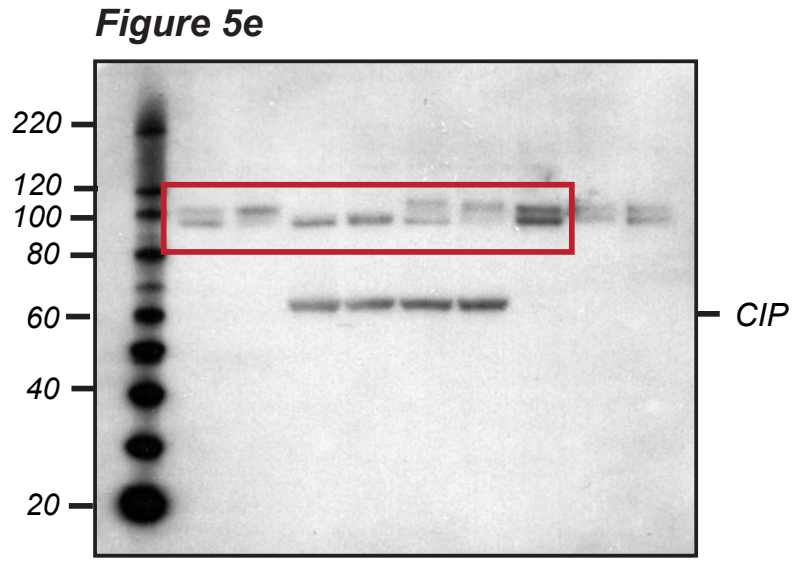

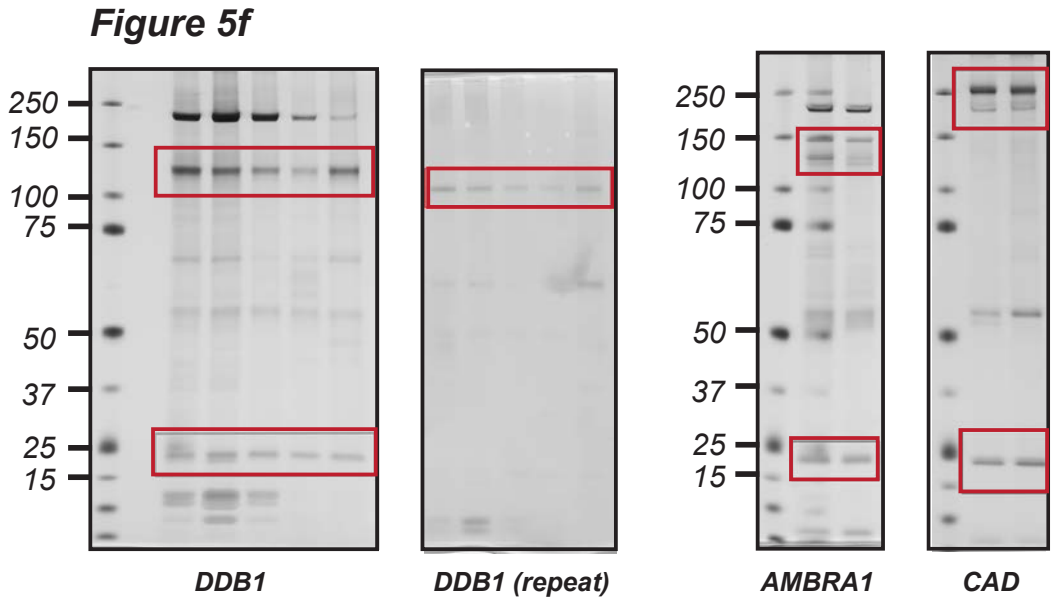

Supplementary Figure 17b. Raw data presentation

DOI: 10.1038/NMICROBIOL.2016.68

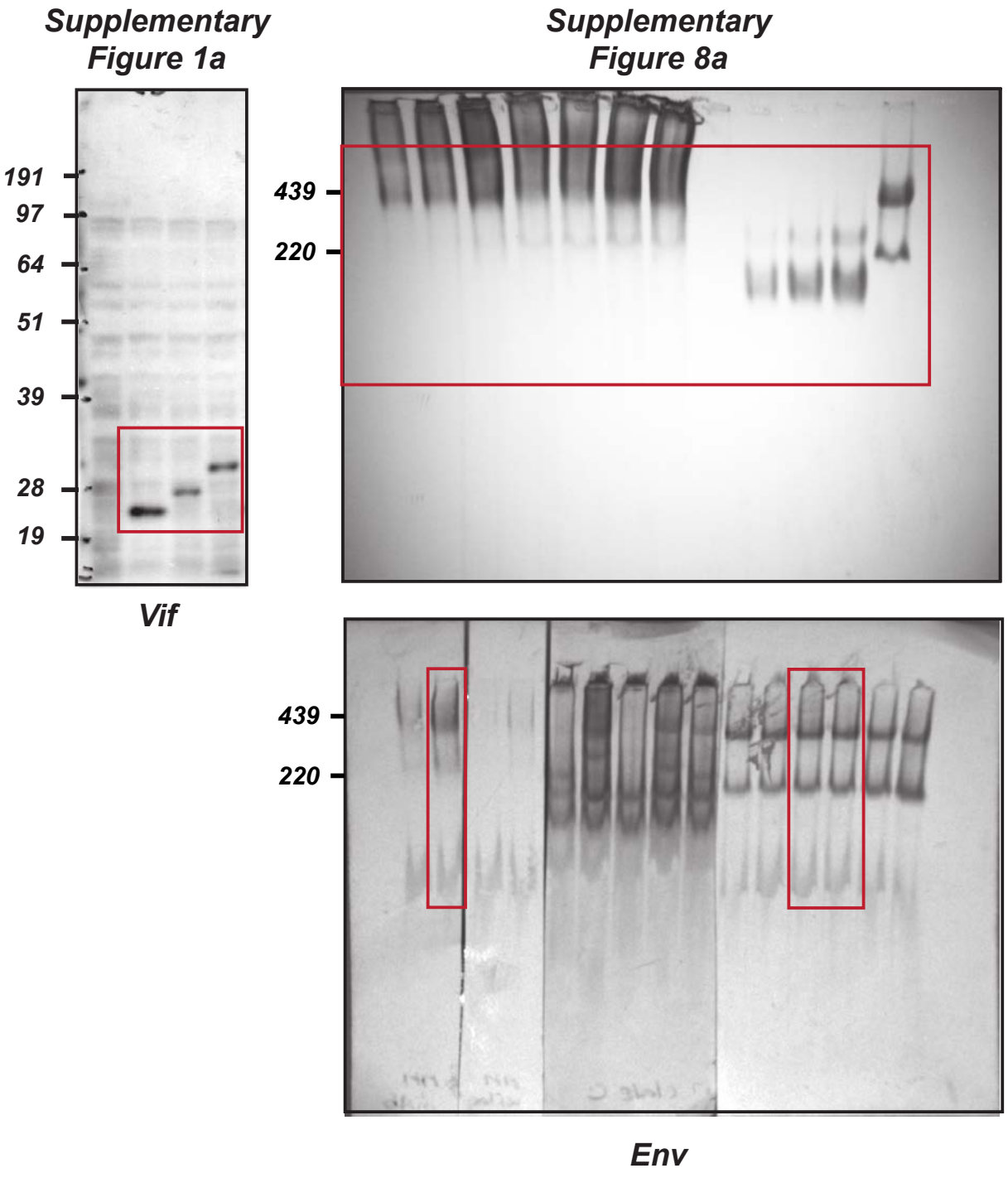

Supplementary Figure 17c. Raw data presentation

UNIPROT ACCESSION	DESCRIPTION	GENE	LENGTH (AA)	IDIRT SPECIFICITY FORWARD	IDIRT SPECIFICITY REVERSE	IDIRT SPECIFICITY AVERAGE	QUANT PSM FORWARD	QUANT PSM REVERSE	TOTAL PSM FORWARD	TOTAL PSM REVERSE	TOTAL PSM SUM	JAGER et al
Q9H497	Torsin-3A	TOR3A	397	0.99	1.00	1.00	12	9	14	15	29	
Q70UQ0	Inhibitor of nuclear factor kappa-B kinase-interacting protein	IKBIP	350	0.99	1.00	1.00	35	20	42	28	70	
P32942	Intercellular adhesion molecule 3	ICAM3	547	0.99	1.00	1.00	9	3	12	5	17	
Q96CG8	Collagen triple helix repeat-containing protein 1	CTHRC1	243	0.99	1.00	1.00	3	7	4	7	11	
P48723	Heat shock 70 kDa protein 13	HSPA13	471	1.00	0.99	1.00	9	10	10	14	24	#
Q8IV08	Phospholipase D3	PLD3	490	0.99	1.00	0.99	4	3	9	3	12	
Q96AQ6	Pre-B-cell leukemia transcription factor-interacting protein 1	PBXIP1	731	0.99	1.00	0.99	59	42	82	57	139	
Q9BWS9	Chitinase domain-containing protein 1	CHID1	393	0.99	1.00	0.99	6	7	7	10	17	
O15533	Tapasin	TAPBP	448	0.99	1.00	0.99	6	6	8	7	15	
P56202	Cathepsin W	CTSW	376	0.99	0.99	0.99	4	7	8	10	18	
P49746	Thrombospondin-3	THBS3	956	0.99	0.99	0.99	41	24	49	27	76	
Q96AE7	Tetratricopeptide repeat protein 17	TTC17	1141	0.99	1.00	0.99	22	11	29	13	42	
Q9Y4L1	Hypoxia up-regulated protein 1	HYOU1	999	0.99	1.00	0.99	179	199	236	318	554	#
P16435	NADPH--cytochrome P450 reductase	POR	677	0.99	1.00	0.99	11	3	13	3	16	
Q9Y287	Integral membrane protein 2B	ITM2B	266	0.99	1.00	0.99	3	3	3	4	7	#
Q15293	Reticulocalbin-1	RCN1	331	0.99	0.99	0.99	8	14	10	18	28	
P05107	Integrin beta-2	ITGB2	769	0.99	1.00	0.99	165	101	221	140	361	
Q9H1E5	Thioredoxin-related transmembrane protein 4	TMX4	349	0.99	1.00	0.99	7	10	10	14	24	
P15814	Immunoglobulin lambda-like polypeptide 1	IGLL1	213	0.99	1.00	0.99	5	7	10	8	18	
O43909	Exostosin-like 3	EXTL3	919	0.99	0.99	0.99	6	4	9	4	13	
P01130	Low-density lipoprotein receptor	LDLR	860	0.99	1.00	0.99	37	30	50	42	92	#
Q02809	Procollagen-lysine,2-oxoglutarate 5-dioxygenase 1	PLOD1	727	0.99	1.00	0.99	3	4	7	4	11	
Q07065	Cytoskeleton-associated protein 4	CKAP4	602	0.99	0.99	0.99	23	15	47	20	67	#
Q8NBJ7	Sulfatase-modifying factor 2	SUMF2	301	0.99	0.99	0.99	10	21	18	50	68	#
Q9UHF1	Epidermal growth factor-like protein 7	EGFL7	273	0.99	1.00	0.99	4	6	4	6	10	
Q4G0T1	Putative scavenger receptor cysteine-rich protein LOC619207	SCART1	1027	0.99	0.99	0.99	36	14	52	19	71	
Q6PKC3	Thioredoxin domain-containing protein 11	TXNDC11	985	0.99	0.99	0.99	7	4	9	5	14	
Q96JJ7	Protein disulfide-isomerase TMX3	TMX3	454	0.99	1.00	0.99	14	12	17	12	29	
P78536	Disintegrin and metalloproteinase domain-containing protein 17	ADAM17	824	0.99	0.99	0.99	3	3	5	3	8	
Q8NBP0	Tetratricopeptide repeat protein 13	TTC13	860	0.99	0.99	0.99	8	5	15	7	22	
O75093	Slit homolog 1 protein	SLIT1	1534	0.99	0.99	0.99	12	5	21	12	33	
Q9NXS2	Glutaminyl-peptide cyclotransferase-like protein	QPCTL	382	0.99	0.99	0.99	5	4	5	6	11	
Q9BZQ6	ER degradation-enhancing alpha-mannosidase-like 3	EDEM3	932	0.99	0.99	0.99	17	9	27	16	43	#
P53634	Dipeptidyl peptidase 1	CTSC	463	0.99	0.99	0.99	3	3	3	3	6	
O00264	Membrane-associated progesterone receptor component 1	PGRMC1	195	0.99	1.00	0.99	4	4	8	7	15	#
P13747	HLA class I histocompatibility antigen, alpha chain E	HLA-E	358	0.99	0.99	0.99	12	8	36	29	65	
Q13087	Protein disulfide-isomerase A2	PDIA2	525	0.99	1.00	0.99	6	9	12	13	25	
P98155	Very low-density lipoprotein receptor	VLDLR	873	0.99	0.99	0.99	9	11	9	13	22	
P03979	T-cell receptor gamma chain V region PT-gamma-1/2	TRGV3	136	0.99	1.00	0.99	5	3	8	4	12	#
O14656	Torsin-1A	TOR1A	332	0.99	1.00	0.99	6	8	9	15	24	#
O60449	Lymphocyte antigen 75	LY75	1722	0.99	0.99	0.99	9	3	12	5	17	
Q5JRA6	Melanoma inhibitory activity protein 3	MIA3	1907	0.99	0.99	0.99	16	16	27	20	47	
A2VDJ0	Transmembrane protein 131-like	KIAA0922	1609	0.99	0.99	0.99	6	4	9	5	14	
Q12907	Vesicular integral-membrane protein VIP36	LMAN2	356	0.99	1.00	0.99	4	12	9	15	24	#
P13674	Prolyl 4-hydroxylase subunit alpha-1	P4HA1	534	0.99	0.99	0.99	4	9	14	11	25	
Q12797	Aspartyl/asparaginyl beta-hydroxylase	ASPH	758	0.99	0.99	0.99	7	3	8	6	14	
P49257	Protein ERGIC-53	LMAN1	510	0.99	0.99	0.99	87	72	140	105	245	#
P80303	Nucleobindin-2	NUCB2	420	0.99	0.99	0.99	12	6	15	8	23	
P05556	Integrin beta-1	ITGB1	798	0.99	0.99	0.99	3	16	7	22	29	
Q92643	GPI-anchor transamidase	PIGK	395	0.99	0.99	0.99	6	3	12	4	16	
O14967	Calmegin	CLGN	610	0.98	1.00	0.99	35	13	40	14	54	#
Q99523	Sortilin	SORT1	831	0.99	0.99	0.99	17	8	20	12	32	
Q13454	Tumor suppressor candidate 3	TUSC3	348	0.99	0.99	0.99	17	12	23	15	38	
Q9BQT9	Calsyntenin-3	CLSTN3	956	0.98	0.99	0.99	14	8	21	14	35	
O75787	Renin receptor	ATP6AP2	350	0.98	1.00	0.99	3	7	3	8	11	
P11717	Cation-independent mannose-6-phosphate receptor	IGF2R	2491	0.99	0.99	0.99	27	9	32	20	52	
Q9UKU9	Angiopoietin-related protein 2	ANGPTL2	493	0.98	0.99	0.99	20	9	28	11	39	
gp160	gp160_Env	gp160	856	0.99	0.98	0.99	586	549	2312	2017	4329	
Q92896	Golgi apparatus protein 1	GLG1	1179	0.98	0.99	0.99	3	3	7	6	13	#
P07766	T-cell surface glycoprotein CD3 epsilon chain	CD3E	207	0.98	0.99	0.99	9	18	13	24	37	
Q96QV1	Hedgehog-interacting protein	HHIP	700	0.98	0.99	0.99	8	7	13	12	25	
Q8NE01	Metal transporter CNNM3	CNNM3	707	0.98	1.00	0.99	10	3	15	4	19	
Q8NBJ5	Procollagen galactosyltransferase 1	GLT25D1	622	0.99	0.98	0.99	13	12	18	19	37	#
O15321	Transmembrane 9 superfamily member 1	TM9SF1	606	0.98	0.99	0.99	8	4	18	10	28	
Q8IWB1	Inositol 1,4,5-triphosphate receptor-interacting protein	ITPRIP	547	0.98	0.99	0.99	4	5	6	7	13	
Q8N766	Uncharacterized protein KIAA0090	KIAA0090	993	0.98	1.00	0.99	11	4	18	7	25	#
Q13586	Stromal interaction molecule 1	STIM1	685	0.98	0.99	0.99	3	9	6	10	16	
Q13724	Mannosyl-oligosaccharide glucosidase	MOGS	837	0.99	0.99	0.99	21	18	32	23	55	#
P30040	Endoplasmic reticulum resident protein 29	ERP29	261	0.98	0.99	0.99	5	12	6	14	20	
P14314	Glucosidase 2 subunit beta	PRKCSH	528	0.98	0.99	0.99	57	42	95	63	158	#
O60568	Procollagen-lysine,2-oxoglutarate 5-dioxygenase 3	PLOD3	738	0.98	1.00	0.99	10	5	11	8	19	
P04234	T-cell surface glycoprotein CD3 delta chain	CD3D	171	0.98	0.99	0.99	6	8	12	10	22	
P27824	Calnexin	CANX	592	0.98	0.99	0.99	140	138	235	185	420	#
P13667	Protein disulfide-isomerase A4	PDIA4	645	0.99	0.99	0.99	35	46	59	73	132	#
Q9Y6M0	Testisin	PRSS21	314	0.99	0.98	0.99	20	13	26	17	43	
P01850	T-cell receptor beta-1 chain C region	TRBC1	177	0.99	0.98	0.99	22	11	29	17	46	#
Q8NFQ8	Torsin-1A-interacting protein 2	TOR1AIP2	470	0.98	0.98	0.98	13	17	23	24	47	#
Q9BRK5	45 kDa calcium-binding protein	SDF4	362	0.98	0.99	0.98	6	9	7	9	16	#
Q9H0U3	Magnesium transporter protein 1	MAGT1	335	0.98	0.98	0.98	26	28	42	36	78	#
P46531	Neurogenic locus notch homolog protein 1	NOTCH1	2555	0.97	0.99	0.98	17	7	32	11	43	
Q9H173	Nucleotide exchange factor SIL1	SIL1	461	0.97	1.00	0.98	4	4	6	5	11	
Q9H3N1	Thioredoxin-related transmembrane protein 1	TMX1	280	0.99	0.97	0.98	40	34	54	54	108	
P07237	Protein disulfide-isomerase	P4HB	508	0.98	0.98	0.98	99	110	162	147	309	#
Q93063	Exostosin-2	EXT2	718	0.99	0.97	0.98	20	4	25	5	30	
Q9BYC5	Alpha-(1,6)-fucosyltransferase	FUT8	575	0.99	0.96	0.98	16	12	32	18	50	#
P49755	Transmembrane emp24 domain-containing protein 10	TMED10	219	0.97	0.98	0.98	25	12	30	16	46	
Q9UH99	SUN domain-containing protein 2	SUN2	717	0.98	0.97	0.98	40	30	62	46	108	
P00387	NADH-cytochrome b5 reductase 3	CYB5R3	301	0.97	0.98	0.98	3	5	5	8	13	
P23229	Integrin alpha-6	ITGA6	1130	0.99	0.96	0.98	12	8	20	11	31	
O94901	SUN domain-containing protein 1	SUN1	812	0.98	0.97	0.97	67	40	89	54	143	#
Q9BTV4	Transmembrane protein 43	TMEM43	400	0.96	0.99	0.97	4	7	5	10	15	#
Q9P2E5	Chondroitin sulfate glucuronyltransferase	CHPF2	772	0.99	0.96	0.97	20	5	33	8	41	
P11021	78 kDa glucose-regulated protein	HSPA5	654	0.97	0.97	0.97	70	79	129	143	272	
P04843	Dolichyl-diphosphooligosaccharide glycosyltransferase	RPN1	607	0.97	0.97	0.97	102	100	159	135	294	#
Q96SL4	Glutathione peroxidase 7	GPX7	187	0.99	0.95	0.97	9	11	9	14	23	
P27797	Calreticulin	CALR	417	0.96	0.98	0.97	44	97	67	140	207	
Q96HE7	ERO1-like protein alpha	ERO1L	468	0.99	0.95	0.97	4	7	9	19	28	
Q8TCJ2	Dolichyl-diphosphooligosaccharide glycosyltransferase	STT3B	826	0.97	0.97	0.97	73	47	98	67	165	
P14625	Endoplasmin	HSP90B1	803	0.97	0.96	0.97	64	110	108	170	278	#
Q9NZ08	Endoplasmic reticulum aminopeptidase 1	ERAP1	941	0.96	0.98	0.97	36	31	46	45	91	
Q9BS26	Endoplasmic reticulum resident protein 44	ERP44	406	0.97	0.97	0.97	18	16	31	24	55	#
Q14697	Neutral alpha-glucosidase AB	GANAB	944	0.97	0.96	0.97	100	73	160	114	274	
Q9HDC9	Adipocyte plasma membrane-associated protein	APMAP	416	0.95	0.98	0.97	4	9	12	11	23	
P30101	Protein disulfide-isomerase A3	PDIA3	505	0.99	0.95	0.97	55	59	72	87	159	#
Q13217	DnaJ homolog subfamily C member 3	DNAJC3	504	0.97	0.96	0.97	12	18	18	28	46	#
P54709	Sodium/potassium-transporting ATPase subunit beta-3	ATP1B3	279	0.94	0.99	0.96	4	4	7	5	12	
Q13438	Protein-9	OS9	667	0.97	0.96	0.96	16	7	26	8	34	#
O96005	Cleft lip and palate transmembrane protein 1	CLPTM1	669	0.96	0.96	0.96	9	8	14	10	24	
Q5JTV8	Torsin-1A-interacting protein 1	TOR1AIP1	583	0.94	0.97	0.96	20	24	33	40	73	
O14672	Disintegrin and metalloproteinase domain-containing protein	ADAM10	748	0.99	0.92	0.95	22	7	27	9	36	
O14524	Transmembrane protein 194A	TMEM194A	444	0.98	0.93	0.95	13	10	18	15	33	
Q9UBS4	DnaJ homolog subfamily B member 11	DNAJB11	358	0.94	0.96	0.95	32	21	57	35	92	#
P39656	Dolichyl-diphosphooligosaccharide glycosyltransferase	DDOST	456	0.95	0.95	0.95	30	19	50	37	87	
Q8IXB1	DnaJ homolog subfamily C member 10	DNAJC10	793	0.96	0.94	0.95	18	11	33	16	49	
Q8TEM1	Nuclear pore membrane glycoprotein 210	NUP210	1887	0.98	0.92	0.95	28	14	39	19	58	
Q14257	Reticulocalbin-2	RCN2	317	0.95	0.94	0.94	10	6	17	13	30	#
O75976	Carboxypeptidase D	CPD	1380	0.89	0.99	0.94	3	4	9	4	13	
Q9HCN8	Stromal cell-derived factor 2-like protein 1	SDF2L1	221	0.95	0.94	0.94	4	7	12	13	25	#
Q9NR31	GTP-binding protein SAR1a	SAR1A	198	0.99	0.89	0.94	3	3	3	8	11	
O43292	Glycosylphosphatidylinositol anchor attachment 1 protein	GPAA1	621	0.99	0.89	0.94	3	5	3	6	9	

Supplementary Table 1a. Env host interactions: list of proteins classified as specific Env interactions by I-DIRT proteomic analysis. Proteins are listed in order of descending I-DIRT specificity ratios, along with the following columns (from left to right): accession/identifier, protein description, gene, protein length in amino acids, I-DIRT specificity in forward and reverse experiments, average I-DIRT specificity, number of peptide spectrum matches (PSM) used for quantification in forward and reverse experiments, total peptide spectrum matches (PSM) in forward and reverse, the sum of peptide spectrum matches and those host proteins (hashtag) jointly identified by Jäger et al.

DOI: 10.1038/NMICROBIOL.2016.68

UNIPROT ACCESSION	DESCRIPTION	GENE	LENGTH (AA)	IDIRT SPECIFICTY FORWARD	IDIRT SPECIFICITY REVERSE	IDIRT SPECIFICITY AVERAGE	QUANT PSM FORWARD	QUANT PSM REVERSE	TOTAL PSM FORWARD	TOTAL PSM REVERSE	TOTAL PSM SUM	JAGER et al
Q32P28	Prolyl 3-hydroxylase 1	LEPRE1	736	0.88	0.99	0.94	6	8	11	9	20	
Q969N2	GPI transamidase component PIG-T	PIGT	578	0.95	0.93	0.94	6	6	14	10	24	
Q9NYU2	UDP-glucose:glycoprotein glucosyltransferase 1	UGGT1	1555	0.95	0.93	0.94	57	32	82	48	130	#
Q96RQ1	Endoplasmic reticulum-Golgi intermediate compartment 2	ERGIC2	377	0.88	0.99	0.94	3	4	6	5	11	#
O43852	Calumenin	CALU	315	0.98	0.88	0.93	7	11	8	16	24	#
P31785	Cytokine receptor common subunit gamma	IL2RG	369	0.94	0.92	0.93	6	3	11	3	14	
Q9BU23	Lipase maturation factor 2	LMF2	707	0.90	0.95	0.93	5	3	9	4	13	
Q8NBS9	Thioredoxin domain-containing protein 5	TXNDC5	432	0.91	0.94	0.93	10	10	15	11	26	#
Q9NTJ5	Phosphatidylinositide phosphatase SAC1	SACM1L	587	0.95	0.90	0.93	17	16	26	28	54	
P51149	Ras-related protein Rab-7a	RAB7A	207	0.93	0.92	0.92	4	14	6	21	27	
Q9UBV2	Protein sel-1 homolog 1	SEL1L	794	0.92	0.93	0.92	18	10	30	19	49	#
Q9BX59	Tapasin-related protein	TAPBPL	468	0.99	0.83	0.91	10	3	14	4	18	
P04844	Dolichyl-diphosphooligosaccharide glycosyltransferase 2	RPN2	631	0.92	0.90	0.91	37	24	73	35	108	
P12268	Inosine-5'-monophosphate dehydrogenase 2	IMPDH2	514	0.91	0.91	0.91	11	9	19	16	35	
P43307	Translocon-associated protein subunit alpha	SSR1	286	0.95	0.87	0.91	6	5	8	8	16	
Q99519	Sialidase-1	NEU1	415	0.89	0.92	0.91	4	3	5	5	10	
Q15392	24-dehydrocholesterol reductase	DHCR24	516	0.86	0.95	0.90	24	10	32	16	48	#
O95573	Long-chain-fatty-acid--CoA ligase 3	ACSL3	720	0.90	0.90	0.90	21	5	39	15	54	
P37268	Squalene synthase	FDFT1	417	0.92	0.88	0.90	19	8	35	18	53	
Q9BSJ8	Extended synaptotagmin-1	ESYT1	1104	0.95	0.85	0.90	16	16	24	22	46	
O95870	Protein BAT5	BAT5	558	0.88	0.90	0.89	6	5	10	8	18	
Q96GQ5	UPF0420 protein C16orf58	C16orf58	468	0.86	0.91	0.89	6	4	12	6	18	
O60831	PRA1 family protein 2	PRAF2	178	0.87	0.87	0.87	8	8	9	15	24	
O75718	Cartilage-associated protein	CRTAP	401	0.83	0.91	0.87	4	3	7	5	12	
Q9Y5M8	Signal recognition particle receptor subunit beta	SRPRB	271	0.89	0.85	0.87	9	19	14	28	42	
P61026	Ras-related protein Rab-10	RAB10	200	0.87	0.87	0.87	3	6	11	20	31	
P55072	Transitional endoplasmic reticulum ATPase	VCP	806	0.90	0.84	0.87	14	13	22	20	42	#
Q8TC12	Retinol dehydrogenase 11	RDH11	318	0.88	0.85	0.87	4	8	9	11	20	
Q6DD88	Atlastin-3	ATL3	541	0.91	0.82	0.86	19	15	26	24	50	#
P02786	Transferrin receptor protein 1	TFRC	760	0.84	0.87	0.86	77	37	137	60	197	
O00231	26S proteasome non-ATPase regulatory subunit 11	PSMD11	422	0.85	0.86	0.85	3	3	7	6	13	#
O43736	Integral membrane protein 2A	ITM2A	263	0.85	0.85	0.85	10	12	19	18	37	
Q15084	Protein disulfide-isomerase A6	PDIA6	440	0.78	0.92	0.85	5	11	12	16	28	
P49411	Elongation factor Tu, mitochondrial	TUFM	452	0.80	0.91	0.85	13	6	20	8	28	
P51571	Translocon-associated protein subunit delta	SSR4	173	0.84	0.86	0.85	3	9	3	15	18	#
Q9UNM6	26S proteasome non-ATPase regulatory subunit 13	PSMD13	376	0.82	0.87	0.84	5	5	8	6	14	
Q96KA5	Cleft lip and palate transmembrane protein 1-like protein	CLPTM1L	538	0.80	0.88	0.84	14	9	22	17	39	
P51148	Ras-related protein Rab-5C	RAB5C	216	0.84	0.83	0.84	3	6	8	15	23	
O75396	Vesicle-trafficking protein SEC22b	SEC22B	215	0.84	0.83	0.84	3	8	5	12	17	
P61106	Ras-related protein Rab-14	RAB14	215	0.83	0.83	0.83	3	8	6	14	20	
Q9Y282	Endoplasmic reticulum-Golgi intermediate compartment 3	ERGIC3	383	0.80	0.85	0.82	11	9	17	11	28	#
Q8TCT9	Minor histocompatibility antigen H13	HM13	377	0.72	0.93	0.82	12	6	17	16	33	#
O00299	Chloride intracellular channel protein 1	CLIC1	241	0.84	0.78	0.81	5	9	6	16	22	
Q8WUM0	Nuclear pore complex protein Nup133	NUP133	1156	0.80	0.82	0.81	3	4	6	7	13	
Q6P1A2	Lysophospholipid acyltransferase 5	LPCAT3	487	0.89	0.71	0.80	8	3	14	5	19	
P13489	Ribonuclease inhibitor	RNH1	461	0.75	0.86	0.80	9	8	17	13	30	
Q93084	Sarcoplasmic/endoplasmic reticulum calcium ATPase 3	ATP2A3	1043	0.78	0.80	0.79	21	8	101	48	149	#
P50402	Emerin	EMD	254	0.82	0.76	0.79	5	7	9	9	18	
Q03519	Antigen peptide transporter 2	TAP2	686	0.87	0.71	0.79	4	3	7	5	12	
Q99460	26S proteasome non-ATPase regulatory subunit 1	PSMD1	953	0.76	0.81	0.79	5	5	7	5	12	
Q9BVC6	Transmembrane protein 109	TMEM109	243	0.83	0.74	0.79	3	3	6	4	10	
P00558	Phosphoglycerate kinase 1	PGK1	417	0.79	0.77	0.78	3	4	9	13	22	
Q9BZF1	Oxysterol-binding protein-related protein 8	OSBPL8	889	0.86	0.70	0.78	3	3	5	5	10	
Q9UBM7	7-dehydrocholesterol reductase	DHCR7	475	0.74	0.80	0.77	23	15	36	28	64	
P17980	26S protease regulatory subunit 6A	PSMC3	439	0.77	0.76	0.76	7	4	10	5	15	
Q53GQ0	Estradiol 17-beta-dehydrogenase 12	HSD17B12	312	0.67	0.85	0.76	4	9	8	13	21	
P35606	Coatomer subunit beta'	COPB2	906	0.81	0.70	0.76	10	7	17	12	29	
P16615	Sarcoplasmic/endoplasmic reticulum calcium ATPase 2	ATP2A2	1042	0.75	0.76	0.75	78	56	198	123	321	#
P62491	Ras-related protein Rab-11A	RAB11A	216	0.77	0.72	0.75	4	6	6	11	17	
P20700	Lamin-B1	LMNB1	586	0.77	0.72	0.75	23	37	51	72	123	
Q13200	26S proteasome non-ATPase regulatory subunit 2	PSMD2	908	0.74	0.75	0.74	16	15	22	25	47	
Q9Y265	RuvB-like 1	RUVBL1	456	0.71	0.77	0.74	11	12	17	19	36	
Q969X5	Endoplasmic reticulum-Golgi intermediate compartment 1	ERGIC1	290	0.71	0.76	0.74	3	4	8	8	16	
Q6P179	Endoplasmic reticulum aminopeptidase 2	ERAP2	960	0.80	0.67	0.74	11	6	16	12	28	
P08575	Receptor-type tyrosine-protein phosphatase C	PTPRC	1304	0.74	0.73	0.73	48	59	89	102	191	
P0CG47	Polyubiquitin-B	UBB	229	0.79	0.66	0.72	35	45	67	83	150	
P15153	Ras-related C3 botulinum toxin substrate 2	RAC2	192	0.73	0.72	0.72	4	8	9	19	28	
P50990	T-complex protein 1 subunit theta	CCT8	548	0.81	0.63	0.72	3	8	9	17	26	
Q96DZ1	Endoplasmic reticulum lectin 1	ERLEC1	483	0.73	0.71	0.72	17	10	30	18	48	#
Q9Y230	RuvB-like 2	RUVBL2	463	0.71	0.73	0.72	11	12	21	16	37	

Supplementary Table 1b. Env host interactions: list of proteins classified as specific Env interactions by I-DIRT proteomic analysis. Proteins are listed in order of descending I-DIRT specificity ratios, along with the following columns (from left to right): accession/identifier, protein description, gene, protein length in amino acids, I-DIRT specificity in forward and reverse experiments, average I-DIRT specificity, number of peptide spectrum matches (PSM) used for quantification in forward and reverse experiments, total peptide spectrum matches (PSM) in forward and reverse, the sum of peptide spectrum matches and those host proteins (hashtag) jointly identified by Jäger et al.

UNIPROT ACCESSION	DESCRIPTION	GENE	LENGTH (AA)	IDIRT SPECIFICTY FORWARD	IDIRT SPECIFICITY REVERSE	IDIRT SPECIFICITY AVERAGE	QUANT PSM FORWARD	QUANT PSM REVERSE	TOTAL PSM FORWARD	TOTAL PSM REVERSE	TOTAL PSM SUM	JAGER et al
Vif3XFLAG	Vif with 3xFLAG insertion	Vif	227	1.00	0.99	1.00	81	81	909	974	1883	
Q13951	Core-binding factor subunit beta	CBFB	182	1.00	0.99	0.99	71	78	349	305	654	#
Q2KJY2	Kinesin-like protein KIF26B	KIF26B	2108	0.99	1.00	0.99	9	5	16	11	27	
O43847	Nardilysin	NRD1	1150	0.98	1.00	0.99	12	5	25	9	34	
Q99707	Methionine synthase	MTR	1265	0.98	1.00	0.99	28	37	60	53	113	
Q86YV9	Hermansky-Pudlak syndrome 6 protein	HPS6	775	0.96	1.00	0.98	7	3	15	8	23	
Pol	Pol polyprotein	Pol	1003	0.97	0.96	0.96	108	35	218	88	306	
Q01113	Interleukin-9 receptor	IL9R	521	0.93	0.98	0.96	18	4	44	23	67	
P46379	Large proline-rich protein BAT3	BAT3	1132	0.91	1.00	0.95	8	4	15	12	27	#
P61221	ATP-binding cassette sub-family E member 1	ABCE1	599	0.96	0.95	0.95	5	8	10	21	31	
P08107	Heat shock 70 kDa protein 1A/1B	HSPA1A	641	0.96	0.94	0.95	9	9	97	86	183	
Q9C0C7	Activating molecule in BECN1-regulated autophagy protein 1	AMBRA1	1298	0.94	0.97	0.95	65	38	170	80	250	#
Q6F5E8	Leucine-rich repeat-containing protein 16C	RLTPR	1435	0.94	0.96	0.95	10	5	23	10	33	
Q5T5P2	Sickle tail protein homolog	SKT	1943	0.89	1.00	0.94	9	4	21	17	38	
P11142	Heat shock cognate 71 kDa protein	HSPA8	646	0.93	0.93	0.93	105	107	720	686	1406	
P30876	DNA-directed RNA polymerase II subunit RPB2	POLR2B	1174	0.94	0.91	0.93	35	26	48	41	89	
Q16531	DNA damage-binding protein 1	DDB1	1140	0.90	0.93	0.91	71	52	149	102	251	
Q15369	Transcription elongation factor B polypeptide 1	TCEB1	112	0.88	0.94	0.91	22	28	90	102	192	#
P04792	Heat shock protein beta-1	HSPB1	205	0.89	0.92	0.91	13	17	43	66	109	
P10809	60 kDa heat shock protein	HSPD1	573	0.90	0.90	0.90	79	55	236	233	469	
P40227	T-complex protein 1 subunit zeta	CCT6A	531	0.90	0.91	0.90	15	11	29	24	53	
Q6UB35	Monofunctional C1-tetrahydrofolate synthase, mitochondrial	MTHFD1L	978	0.92	0.88	0.90	29	12	71	52	123	
P35869	Aryl hydrocarbon receptor	AHR	848	0.85	0.94	0.89	10	8	18	17	35	
Q15370	Transcription elongation factor B polypeptide 2	TCEB2	118	0.86	0.92	0.89	29	21	123	96	219	#
P78371	T-complex protein 1 subunit beta	CCT2	535	0.89	0.88	0.89	15	11	26	14	40	
P50990	T-complex protein 1 subunit theta	CCT8	548	0.87	0.90	0.89	28	10	50	24	74	
O15067	Phosphoribosylformylglycinamidine synthase	PFAS	1338	0.80	0.97	0.88	7	3	14	7	21	
Q99832	T-complex protein 1 subunit eta	CCT7	543	0.91	0.85	0.88	15	12	26	24	50	
P48643	T-complex protein 1 subunit epsilon	CCT5	541	0.87	0.89	0.88	18	14	33	31	64	
P52732	Kinesin-like protein KIF11	KIF11	1056	0.93	0.83	0.88	4	7	9	12	21	
P50991	T-complex protein 1 subunit delta	CCT4	539	0.86	0.89	0.88	17	16	41	36	77	
Q7Z6Z7	E3 ubiquitin-protein ligase HUWE1	HUWE1	4374	0.85	0.90	0.88	53	35	124	75	199	#
P27708	CAD protein	CAD	2225	0.83	0.92	0.87	57	42	142	91	233	
Q13765	Nascent polypeptide-associated complex subunit alpha	NACA	215	0.84	0.91	0.87	5	3	9	7	16	
P49368	T-complex protein 1 subunit gamma	CCT3	545	0.88	0.86	0.87	24	11	44	29	73	
Q5VV42	CDK5 regulatory subunit-associated protein 1-like 1	CDKAL1	579	0.80	0.93	0.86	4	4	8	7	15	
P40939	Trifunctional enzyme subunit alpha, mitochondrial	HADHA	763	0.86	0.86	0.86	13	5	33	14	47	
P49327	Fatty acid synthase	FASN	2511	0.85	0.86	0.86	49	20	102	54	156	
P24928	DNA-directed RNA polymerase II subunit RPB1	POLR2A	1970	0.94	0.77	0.85	13	9	23	25	48	
P17987	T-complex protein 1 subunit alpha	TCP1	556	0.82	0.88	0.85	23	12	41	33	74	
O60884	DnaJ homolog subfamily A member 2	DNAJA2	412	0.80	0.89	0.84	11	5	34	31	65	
Q9NSE4	Isoleucyl-tRNA synthetase, mitochondrial	IARS2	1012	0.83	0.86	0.84	11	5	19	8	27	
P46821	Microtubule-associated protein 1B	MAP1B	2468	0.77	0.91	0.84	8	6	33	26	59	
P22102	Trifunctional purine biosynthetic protein adenosine-3	GART	1010	0.74	0.94	0.84	7	5	14	11	25	
Q8N163	Protein KIAA1967	KIAA1967	923	0.72	0.95	0.83	11	3	22	6	28	
Q5SW79	Centrosomal protein of 170 kDa	CEP170	1584	0.81	0.84	0.82	6	3	13	5	18	
P07900	Heat shock protein HSP 90-alpha	HSP90AA1	732	0.82	0.83	0.82	8	5	186	118	304	
Q9UKT9	Zinc finger protein Aiolos	IKZF3	509	0.84	0.80	0.82	11	5	22	13	35	
P02786	Transferrin receptor protein 1	TFRC	760	0.78	0.85	0.82	13	3	31	14	45	
O95831	Apoptosis-inducing factor 1, mitochondrial	AIFM1	613	0.78	0.84	0.81	15	9	32	17	49	
Q9NNW5	WD repeat-containing protein 6	WDR6	1121	0.80	0.83	0.81	7	3	12	10	22	
P31689	DnaJ homolog subfamily A member 1	DNAJA1	397	0.78	0.83	0.81	19	13	77	48	125	
Pr55	Gag Pr55 Gag precursor (Assemblin)	Pr55	500	0.82	0.79	0.81	73	37	170	129	299	
Q08AF3	Schlafen family member 5	SLFN5	891	0.72	0.90	0.81	5	3	20	11	31	
O75616	GTP-binding protein era homolog	ERAL1	437	0.76	0.85	0.80	5	4	6	7	13	
Q13617	Cullin-2	CUL2	745	0.65	0.89	0.77	65	43	156	121	277	#

Supplementary Table 2. Vif host and viral interactions: list of proteins classified as specific Vif interactions by I-DIRT proteomic analysis. Proteins are listed in order of descending I-DIRT specificity ratios, along with the following columns (from left to right): accession/identifier, protein description, gene, protein length in amino acids, I-DIRT specificity in forward and reverse experiments, average I-DIRT specificity, number of peptide spectrum matches (PSM) used for quantification in forward and reverse experiments, total peptide spectrum matches (PSM) in forward and reverse, the sum of peptide spectrum matches and those host proteins (hashtag) jointly identified by Jäger et al.